



Soil erosion vulnerability and soil loss estimation for Siran River watershed, Pakistan: an integrated GIS and remote sensing approach

Mehwish Mehwish · Muhammad Jamal Nasir ·
Abdur Raziq · Ayad M. Fadhil Al-Quraishi ·
Fadhil Ali Ghaib

Received: 30 July 2023 / Accepted: 14 December 2023 / Published online: 30 December 2023
© The Author(s), under exclusive licence to Springer Nature Switzerland AG 2023

Abstract Soil erosion is a problematic issue with detrimental effects on agriculture and water resources, particularly in countries like Pakistan that heavily rely on farming. The condition of major reservoirs, such as Tarbela, Mangla, and Warsak, is crucial for ensuring an adequate water supply for agriculture in Pakistan. The Kunhar and Siran rivers flow practically parallel, and the environment surrounding both rivers' basins is nearly identical. The Kunhar River is one of KP's dirtiest rivers that carries 0.1 million tons of suspended sediment to the Mangla reservoir. In contrast, the Siran River basin is largely unexplored. Therefore, this study focuses on the Siran River

basin in the district of Manshera, Pakistan, aiming to assess annual soil loss and identify erosion-prone regions. Siran River average annual total soil loss million tons/year is 0.154. To achieve this, the researchers integrate Geographical Information System (GIS) and remote sensing (RS) data with the Revised Universal Soil Loss Equation (RUSLE) model. Five key variables, rainfall, land use land cover (LULC), slope, soil types, and crop management, were examined to estimate the soil loss. The findings indicate diverse soil loss causes, and the basin's northern parts experience significant soil erosion. The study estimated that annual soil loss from the Siran River basin is 0.154 million tons with an average rate of 0.871 tons per hectare per year. RUSLE model combined with GIS/RS is an efficient technique for calculating soil loss and identifying erosion-prone areas. Stakeholders such as policymakers, farmers, and conservationists can utilize this information to target efforts and reduce soil loss in specific areas. Overall, the study's results have the potential to advance initiatives aimed at safeguarding the Siran River watershed and its vital resources. Protecting soil resources and ensuring adequate water supplies are crucial for sustainable agriculture and economic development in Pakistan.

M. Mehwish · M. J. Nasir
Department of Geography, University of Peshawar,
Peshawar, Pakistan
e-mail: meshii9696@gmail.com

M. J. Nasir
e-mail: drjamal@uop.edu.pk

A. Raziq
Department of Geography, Islamia College Peshawar,
Peshawar, Pakistan
e-mail: drraziq@icp.edu.pk

A. M. F. Al-Quraishi (✉) · F. A. Ghaib
Petroleum and Mining Engineering Department, Tishk
International University, Erbil 44001, Kurdistan Region,
Iraq
e-mail: ayad.alquraishi@tiu.edu.iq

F. A. Ghaib
e-mail: fadhil.ali@tiu.edu.iq

Keywords RUSLE model · Remote sensing · GIS ·
Soil erosion · Siran River · Pakistan

Introduction

Water erosion is responsible for a significant portion of the estimated $2000 \text{ t km}^{-2} \text{ year}^{-1}$ of topsoil removal, making it a primary contributor to global soil erosion (Cherif et al., 2023). Intense precipitation, rushing rivers, and other water-related activities contribute to soil surface erosion, which is transported downstream. This has far-reaching consequences for agriculture, human activities dependent on fertile soil, and the health of aquatic ecosystems downstream. While less frequent, wind erosion can also substantially impact, particularly in desert regions where the top layer of soil is susceptible to being carried away by strong wind gusts due to limited moisture availability (Chuenchum et al., 2020; Fadhil, 2013). Soil erosion is a significant concern that will persist in the future, particularly in low and middle-income countries, notably in tropical and sub-tropical region (Lal, 2001). Each year, water and wind erosion damage approximately 1.094 and 0.549 billion hectares of land, respectively (Lal, 2003). Evaluating and predicting soil loss is a crucial subject in soil science. It is a joint exercise to predict soil loss rates and calculate the transport sediment production using RUSLE (Gayen et al., 2020; Liou et al., 2022; Neupane et al., 2023).

As a consequence of anthropogenic activities, including shifting land uses, woodland loss, excessive grazing, and intensive farming practices, soil erosion has become a significant environmental issue that has worsened during the twentieth century (Hossini et al., 2022; Tiruneh and Ayalew, 2015; Meadows, 2003). In addition, climate change is also a contributing factor that alters precipitation patterns, causing more intense rainfall and increasing the risk of soil erosion (Li & Fang, 2016). Steep slopes and shallow soils are particularly at risk of soil erosion, making them more vulnerable to aeolian and fluvial erosion (Mahala, 2020). Soil erosion is a complicated problem that requires a multi-faceted approach, including implementing erosion control practices measures, such as building check dams and ecological restoration to alleviate climate change effects by enhancing agricultural system resilience, and sustainable land use exercises (Ashraf et al., 2017; Hoyos, 2005; Pradeep et al., 2015; Yuliang & Yun, 2002).

Park et al. (2011) emphasize the significance of quantities analysis in assessing soil erosion risk and determining efficient control of erosion techniques.

This approach facilitates measuring and anticipating soil erosion rates, enabling informed land management choices and prioritizing conservation endeavors. Fluvial erosion is harmful to agricultural productivity as it removes the topmost fertile soil layer containing organic material and critical nutrients for plant growth. Every year, 75 billion tons of soils are lost from agricultural land around the world (Akça et al., 2022). There are locations and circumstances where fluvial erosion rates exceed $100 \text{ t ha}^{-1} \text{ year}^{-1}$ (Osman & Osman, 2014). Consequently, crop production may be impacted. Loss of soil structure and decreased soil fertility ultimately affect food security and ecosystem health. Therefore, stopping soil erosion and promoting acceptable land management exercises are essential to maintain healthy soil and productive agricultural land (Bag et al., 2022; Gilani et al., 2022; Luetzenburg et al., 2020; Piacentini et al., 2018).

Soil erosion modeling is a valuable tool for evaluating erosion's magnitude and spatial distribution, providing crucial insights for guiding land-use decisions and implementing effective management strategies to mitigate its impacts (Mitasova et al., 2013; Toubal et al., 2018). Using diverse models, including the RUSLE model and its derivatives, researchers and land managers can estimate erosion rates, patterns, and those underlying issues contributing to soil erosion over extensive land. This approach also enables the identification of erosion hotspots, i.e., areas with severe soil erosion (Gelagay & Minale, 2016). Developing appropriate land-use strategies and practices, i.e., conservation farming, contour cropping, and terracing, becomes feasible using erosion-susceptible area maps generated through these models. These measures aim to prevent soil loss while preserving the fertility of soils (Karydas et al., 2020; Millington, 1986; Xie et al., 2021). Ricci et al. (2020) undertook a study to identify effective Best Management Practices (BMPs) to minimize soil erosion in the Puglia region of Italy. Four management scenarios were implemented: contour farming (BMP1), no-tillage (BMP2), reforestation (BMP3), and contour farming with reforestation (BMP4). Combining contour farming and reforestation (BMP4) was shown to be the most effective method, resulting in a 38% reduction in soil erosion (from 5.95 to 3.70 t ha^{-1}) followed by BMP2 (29%), BMP1 (22%), and BMP3 (15%).

Identifying factors contributing to soil detachment is paramount when designing erosion control

measures (Hossini et al., 2022). The RUSLE model is widely employed in soil erosion modeling due to its efficiency and straightforwardness. This model incorporates five crucial variables, namely rainfall, soil type, steepness, slope length, LULC management, and calculation of soil erosion with support practice. GIS/RS data sets can be used to estimate these variables in different forms. By considering these physical variables, the RUSLE model allows the creation of continuous soil erosion prediction (Biswas & Pani, 2015; Habtu & Jayappa, 2022).

Pakistan is confronted with various challenges encompassing natural hazards, socio-economic development, and the repercussions of climate change. It is situated in a geographically precarious region. The country frequently experiences natural calamities, i.e., floods, drought, landslides, and earthquakes. These calamities substantially impact Pakistan's economy and infrastructure, resulting in loss of life, displacement of people, and damage to property and agriculture (Gilani et al., 2022). According to the Global Climate Risk Index, Pakistan was the fifth most vulnerable to climate change in light of its vulnerability to environmental hazards and its capacity to manage and adapt to these risks (Eckstein et al., 2019).

Fluvial erosion is an important ecological concern in Pakistan. It contributes to poor water quality by carrying suspended sediment and pollutants in river water. These consequences extend beyond the immediate site, including sediment deposition in reservoirs, reduced water storage capacity, and equipment damage. These environmental impacts have significant economic and social implications for the population (Swarnkar et al., 2018; Walling, 1983). Erosion occurring in the young mountains of Hindukush, Himalayas, and Karakorum substantially contributes to carrying sediment load by River Indus. Consequently, the sediment eventually accumulates in the Tarbela Dam. On average, the Indus River transports approximately 250 million tons of silt annually (Kalhor et al., 2021). Understanding the reason for soil loss is crucial to growing actual erosion management strategies. Moreover, identifying erosion-prone areas can help prioritize conservation efforts (Arabameri et al., 2018). The significant effects of sedimentation in reservoirs underscore the importance of soil erosion management to ensure sustainable water and

energy resources, food security, and environmental well-being.

The economic, food security, and ecosystem implications of sedimentation and siltation in reservoirs are substantial. Specifically, in the context of Pakistan, the loss of capacity in the Tarbela reservoir due to sedimentation can adversely affect hydropower production, water supply, agricultural productivity, and fisheries in downstream regions. Moreover, the impacts of sedimentation on shared rivers between Pakistan and neighboring countries can give rise to cross-border conflicts over water resources (Ul-Hussan et al., 2020). The prime objectives are: (1) To recognize the key factors contributing to soil erosion within the research area. (2) To delineate areas that are particularly vulnerable to erosion. (3) To understand the RUSLE model efficiency in soil loss estimation.

Materials and methods

Study area

The Mansehra District, in the Hazara Division of Khyber Pakhtunkhwa Province, Pakistan encompassing a total area of 4,125 km², is home to an estimated population of 1,555,742 residents as per the 2017 census. This population density equates to approximately 377.15 people per km². Between 1998 and 2017, the district exhibited an average annual growth rate of 2.47%. Geographically, the district (Fig. 1) is situated within the coordinates of latitude 34°14'05" to 35°11'15" N and longitude 72°09'10" to 72°48'15" E. It shares borders with Muzaffarabad district to the east, Kohistan and Battagram districts to the north, Abbottabad and Haripur districts to the south, and Shangla and Buner districts to the west. The district's strategic location holds significant importance in tourism and transportation (Arif et al., 2022).

The Karakoram Highway, traversing through the district, is a major transportation route connecting Pakistan with China to the northern region and acts as a getaway between these two countries. Due to its diverse topography and location, the district serves as a catchment area for several significant valleys, including Kaghan, Batagram, and Balakot (Inam, 2021). Effectively managing soil erosion and other environmental concerns in this area is crucial to

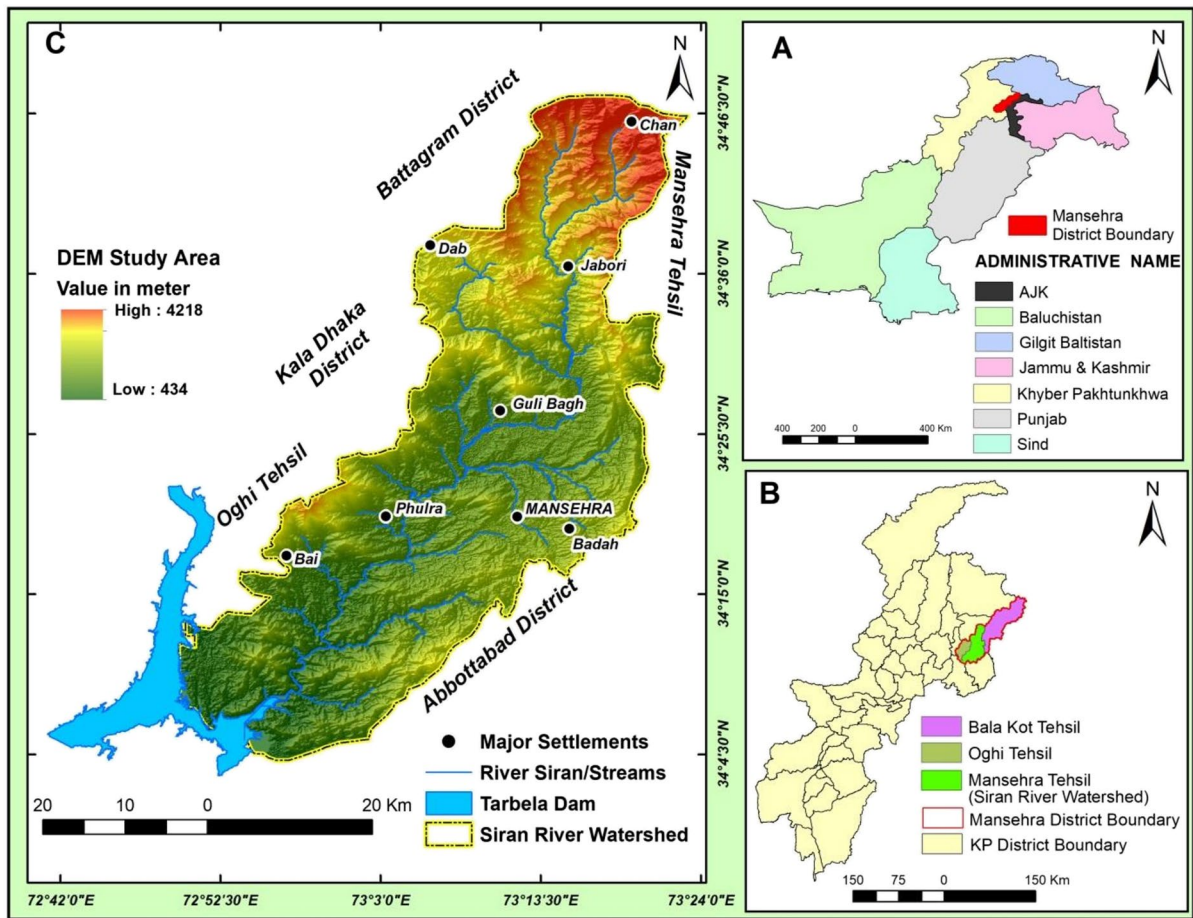


Fig. 1 A Pakistan administrative map. B Khyber Pakhtunkhwa map and location of Mansehra district, and location of Siran River Watershed. C The location of Siran River watershed

ensure sustainable development and preserve its natural beauty. Mansehra district encounters diverse climatic conditions, encompassing winter snowfall and heavy rainfall during the monsoon season.

Notably, maize and wheat are the primary crops cultivated in the district, contributing significantly to its agricultural production (Ahmad et al., 2007; Khwaja et al., 2018). The Kunhar and Siran rivers are crucial in providing water resources for the district. Originating from the enchanting Lake Saif-ul-Malook, the Kunhar River traverses Balakot and Garhi Habibullah before joining the Neelum River (Taneez et al., 2021). On the other hand, the Siran River originates from the Mandagucha Glacier and meanders through the Pakhal Valley, ultimately flowing into the Tarbela Dam. Two significant canals, namely the Siran Canal at Dharial

in the upper part and Siran Canal at Shinkari in the lower part, have been constructed along the course of the Siran River, serving as vital irrigation channels (Qaisar et al., 2008; Raza et al., 2016).

The watershed of Siran River is situated within the latitude range of $34^{\circ}34'30''$ and $34^{\circ}45'15''$ and the longitude range of $73^{\circ}15'30''$ and $73^{\circ}25'15''$ east. Stretching approximately 130 km, the river joined with the Indus River at Tarbela in the Hazara division. Siran River catchment exhibits diverse landscapes comprising valleys, mountains, plains, and lakes. The geological formations in the region encompass a broad period, ranging from the Precambrian age to the present era, and exhibit remnants of both Cambrian and Precambrian rocks (Awan et al., 2021).

Methodology

The prime goal of this research is to estimate soil loss resulting from water erosion using the RUSLE model, which incorporates multiple factors associated with soil erosion. To achieve this objective, it encompassed activities such as data collection, data processing and analysis, generation of RUSLE factors maps, creation of a soil erosion risk map, and analysis and discussion of results. The methodology flow diagram is presented in Fig. 2.

This study employed the RUSLE model based on secondary data sources to determine the average annual soil loss. This model considers several important factors to estimate soil loss, i.e., rainfall, soil type, slope length, steepness, maintenance factor, and LULC management. The RUSLE model

is empirically defined as follows (Renard et al., 1996):-

$$A = R \times K \times LS \times C \times P \tag{1}$$

where,

A = yearly mean soil loss (t/ha every year)

R = precipitation erodibility factor (MJ/ha every year)

K = soil erodibility factor (t ha h MJ⁻¹mm⁻¹)

LS = slope length and slope steepness factor

C = cover management factor

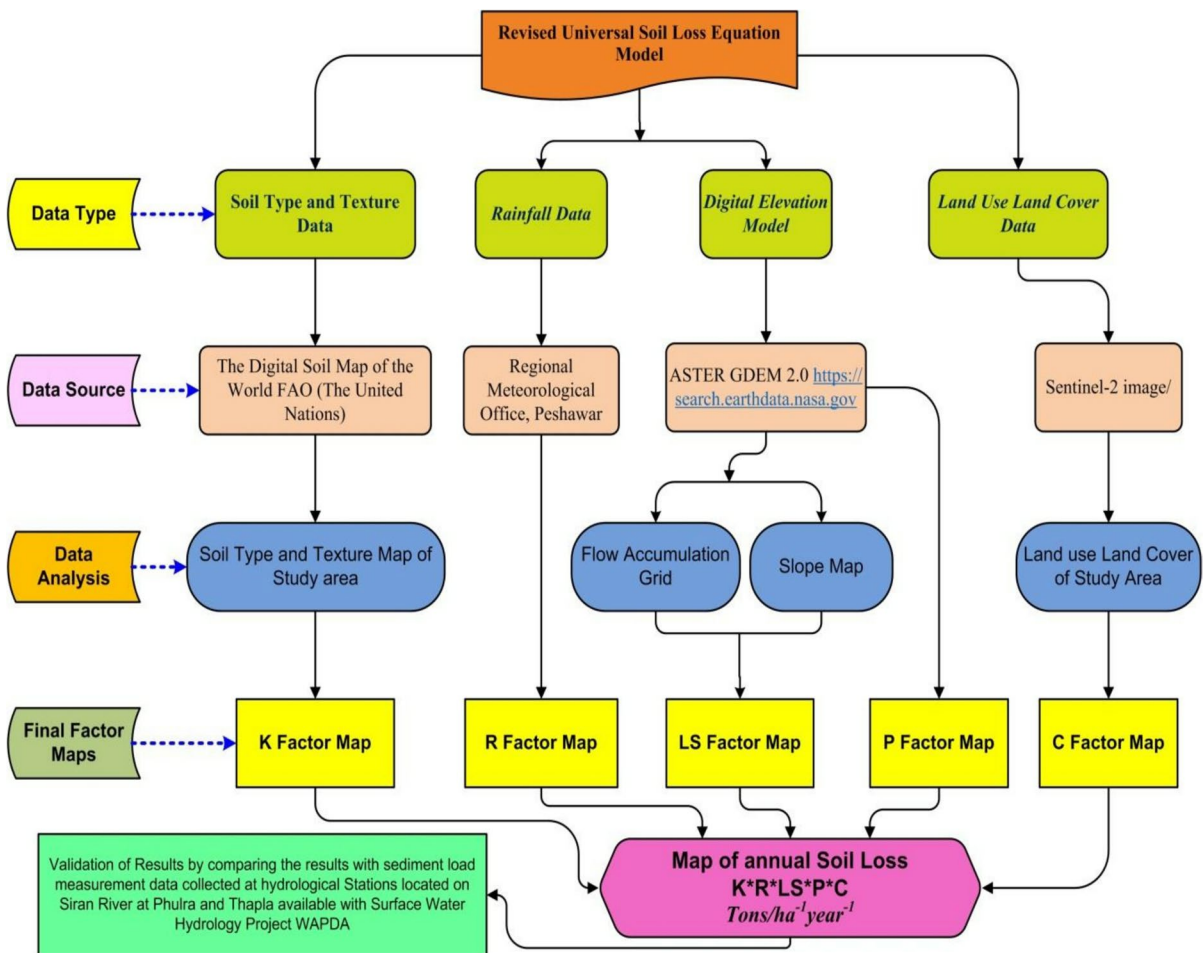


Fig. 2 The methodology flow diagram

P = support practice factor

Rainfall erosivity (R) factor

The influence of runoff is considered while calculating R factor, determining the power of rainfall on soil erosion. According to Wischmeier and Smith (1978) and Cardoso et al. (2020), the value of R-factor for a given rainfall event is determined by multiplying the rainfall energy (E) by 30-min rainfall intensity (I-₃₀) in millimeters per hour. The rainfall impact on soil loss is acknowledged by various factors, counting the intensity and amount of rainfall, duration, size, and raindrop distribution (Jadhao et al., 2023; Yan et al., 2008; Ziadat & Taimeh, 2013).

However, estimating rainwater erosivity can pose challenges, particularly in regions where long-term rainfall data is not readily available, including specific areas of Pakistan. Simplified approaches have been developed to overcome this limitation, utilizing easily accessible meteorological information to predict the R-factor. These models establish statistical relationships between precipitation characteristics, such as intensity, duration, frequency, and rainfall erosivity. Although these simplified models may not capture the full range of erosivity variability, they can provide valuable estimations of rainfall erosivity factor in data-scarce regions. The precision of these approaches may vary depending on local climatic conditions and should be validated through field measurements whenever possible (Morgan, 2009). Panagos et al. (2017) used Global rainfall erosivity database to prepare erosivity map at 30 arc Second based on gaussian process regression.

Several studies have utilized annual rainfall data to compute the erosivity factor (R), such as Awan et al. (2021), Aslam et al. (2021), Chen et al. (2022), Patriche et al. (2023), Angulo-Martínez and Beguería (2009), Panagos, Ballabio, et al. (2015a), and Panagos et al. (2017). In this study, Eq. 2 was employed due to its simplicity, as supported by Chuenchum et al. (2020), Aslam et al. (2021), Musabbir et al. (2023) (Ghosal & Das, 2020), (Maurya & Tanwar, 2021), and (Li et al., 2022).

$$R = 79 + 0.363 \times AAP \quad (2)$$

where R represents the factor of rainfall erosivity, while AAP is the average annual rainfall.

Rainfall data for the meteorological stations of Kakul (Abbottabad), Haripur, and Balakot has been collected over 20 years from 2000 to 2020. The

gathered data was organized in an attribute table and linked to a location map of the meteorological stations. The Kriging technique was utilized to interpolate point data and generate a continuous surface. Subsequently, the masking tool was used to acquire rainfall data from the interpolated surface of a specific study area (Usovicz et al., 2021).

Soil erodibility (K) factor

Wischmeier et al. (1971) defined “soil erodibility” as the innate propensity of soil eroded by water or wind. It is referred to as a K-factor, the quantities measurement of the resistance to soil erosion. Different soil types may show varied degrees of erosive sensitivity. A variety of physiochemical characteristics of soil affect how easily it erodes, and these characteristics, taken as a whole, can show how resistant the soil is to erosion from surface runoff and rainfall (Khan, 2021). Two physical variables that could influence the K-factor are soil texture, which defines the proportions of sand, silt, and clay components in soil, and soil structure, which specifies how the soil components are grouped into clusters. Soil compaction, slope steepness and length, and vegetation cover can also impact soil erodibility. Additionally, soil’s chemical characteristics, including organic matter content, nitrogen levels, and pH, might impact soil erodibility.

According to Kim et al. (2012), a K-factor value is provided for a specific type of soil type on a conventional study parcel (22.18 m length, 1.83 m width, with a slope gradient is 9%). Typically, the K-factor’s value ranges from 0.01 to 1. To calculate the value of the K-factor for different soil types, Eq. 3 was used by Sharpley & Williams, 1990 in the current study. Data was downloaded from the website (<https://www.fao.org/soils-portal/soil-survey/soil-maps-and-databases/faunesco-soil-map-of-the-world>) to account for soil types in the research region.

$$K = fcsand \times fcl-si \times forgc \times fhisand \quad (3)$$

where, fcsand, fcl, forg, and fhisand represent a fraction of coarse sand, a fraction of clay, a fraction of organic matter, and a fraction of sand in the soil, respectively. The fcsand has a low soil erodibility factor, while the factor for soil with high coarse content and less sand content has a high value for soil. The clay and silt having a high proportion ratio in

the soil produced by fcl-si result in low soil erosion. High organic matter content in the soil, as indicated by the forgc percentage, leads to reduced soil erosion, particularly in soils with an exceptionally high sand proportion.

$$fcsand = (0.2 + 0.3 \times \exp) - 0.256 \times ms \times \left(1 - \frac{msilt}{100}\right) \tag{3.1}$$

$$fcl - si = \left[\frac{msilt}{mc + msilt}\right] 0.3 \tag{3.2}$$

$$forgc = \left[1.0 - \frac{0.25 \times orgc}{orgc + \exp[(3.72 - 2.95 \times orgc)]}\right] \tag{3.3}$$

$$fhisans = 1 - \frac{0.7 \times \left(1 - \frac{ms}{100}\right)}{\left(1 - \frac{ms}{100}\right) + \exp\left(-5.51 + 22.9 \times \left(1 - \frac{ms}{100}\right)\right)} \tag{3.4}$$

where, ms and msilt are the percent sand and silt content with a diameter particle of 0.05–20 mm and 0.02–0.05 mm. While on the other hand, mc and orgc are the percent of clay and organic matter of content with a diameter particle less than 0.002 mm and soil layer in %, respectively. The DSMW was used to obtain the texture of soil data, i.e., sand, silt, clay, and organic material proportions for the study area mentioned earlier. Subsequently, MS Excel was used for the calculation of each type of soil erodibility.

Slope length and steepness factor (LS)

The length of slope and gradient is crucial in soil erosion, affecting LS factor (Chauhan et al., 2020; Khan, 2021). The soil erosion proportion is significantly influenced by terrain’s characteristics, particularly the length of slope and gradient. Steeper slopes are more vulnerable to erosion due to the water runoff of higher velocity, exerting greater pressure on the topsoil. (Chauhan et al., 2020; Khan, 2021).

In addition to steep gradients, longer slope lengths increase soil erosion as rainwater has more time to erode the soil. To determine the LS factor, an effective approach is to utilize a digital elevation model (DEM) (Chauhan et al., 2020; Khan, 2021). In the present investigation, the LS factor was determined using Moore and Burch (1986)’s algorithm (Eq. 4) with the aid of the 30-m ASTER GDEM (Chauhan

et al., 2020). This factor is essential for estimating soil loss and understanding erosion dynamics (Chauhan et al., 2020; Khan, 2021).

$$LS = \frac{(slope\ length)^{0.4}}{22.13} \times \frac{(0.01745 \sin\theta^{1.4})}{0.0896} \times 1.4 \tag{4}$$

where the length of the slope is a flow of accumulation \times Digital elevation model cell size used and θ = degree in slope.

The slope length is calculated using the slope percentage and size of pixel of the digital elevation model. Arc-Hydro tool of ArcMap 10.8 was utilized to create accumulation flow from DEM. Das (2021) point out that factor of LS increases as slope length and gradient increase. Areas where flow accumulation takes place are identified as highly vulnerable to soil loss and erosion.

Cover and management factor (C)

In soil erosion simulation, the C-factor represents crop cover and management practices, encompassing the influence of crop cultivation, vegetative cover, and soil erosion mitigation techniques on soil loss. When the land lacks vegetation and is bare, the C-factor is typically assigned a value of 1.0, indicating a lack of protection against soil erosion. However, as vegetative cover increases, the C-factor decreases, signifying greater protection against soil erosion (Egbueri et al., 2022; Obiahu & Elias, 2020; Rawat & Singh, 2018). It is worth noting that when water bodies are considered, the C-factor is often assigned a value of 0 since there is no soil to preserve in such areas. Additionally, vegetation plays a vital role in regulating the erosive force of raindrops. When vegetation covers the soil, it acts as a barrier, preventing raindrops from directly impacting the soil surface and slowing down their erosive effect. Therefore, maintaining a healthy vegetation cover is essential for reducing soil erosion and preserving soil health (Erenstein, 1999).

Sentinel-2 images with a 10-m spatial resolution were acquired from the USGS website and analyzed using ArcGIS 10.8 to determine the C-factor. Maximum likelihood supervised classification was applied to analyze the images into LULC classes. The classified image has been rationalized and evaluated using open-source Google Earth Pro. The accuracy was evaluated for overall accuracy and Kappa coefficient.

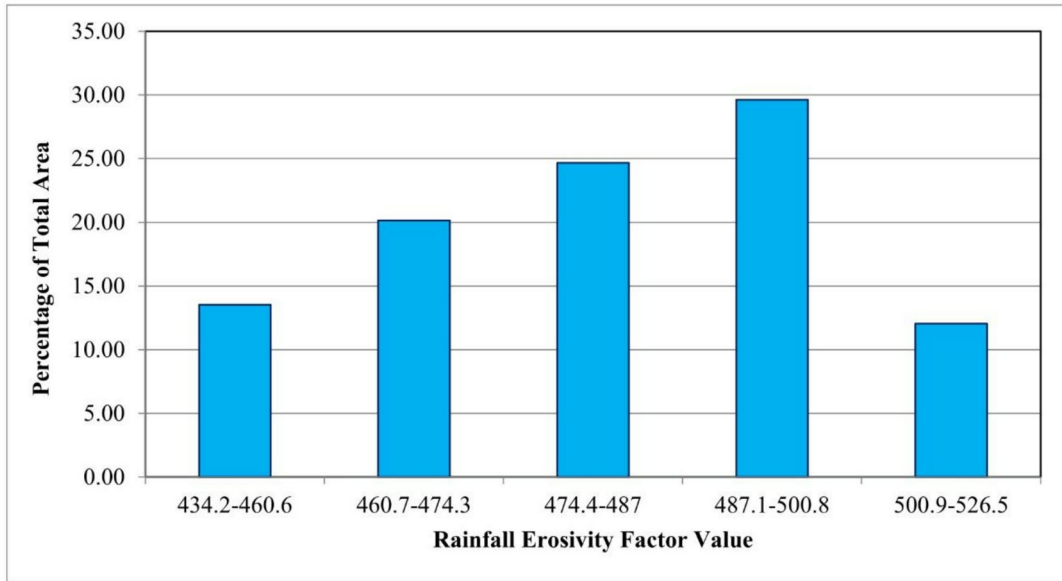


Fig. 3 R-factor classes and associated area under class in the Siran Basin

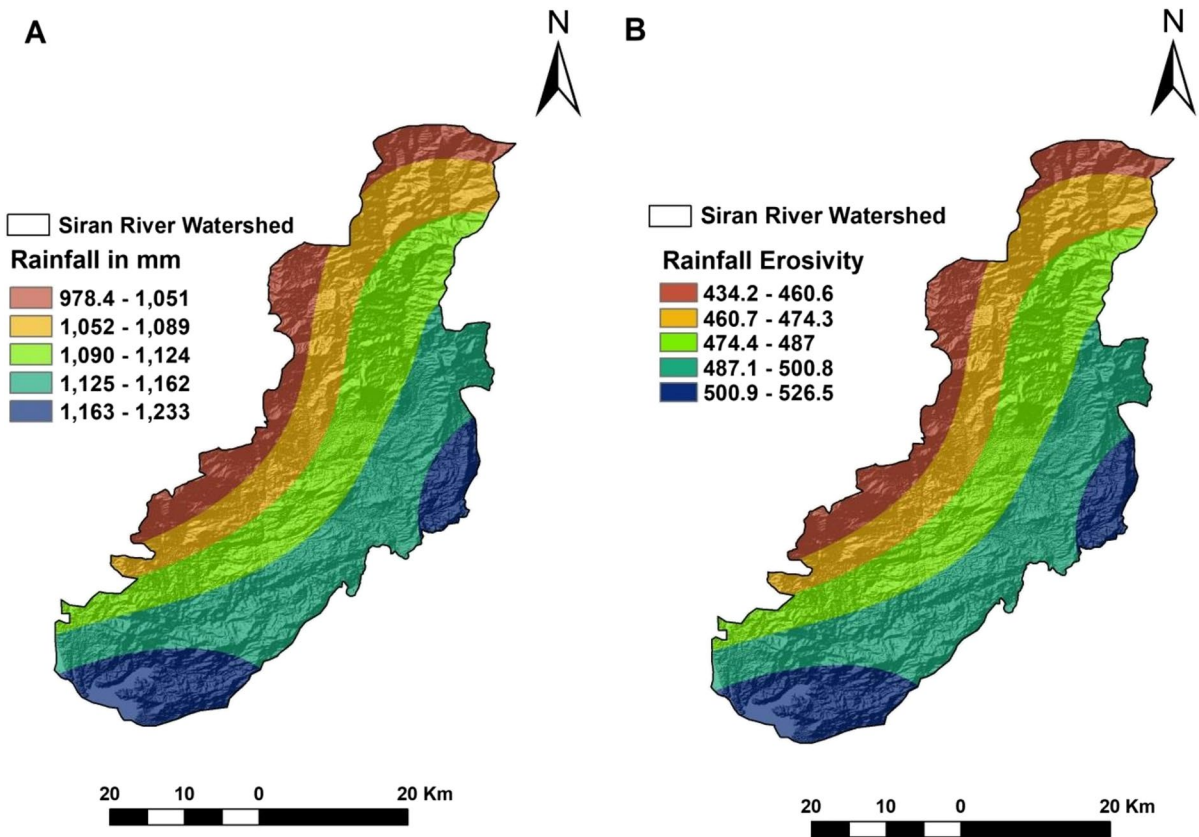


Fig. 4 A Mean annual rainfall in mm. B Rainfall erosivity factor map. C Pakistan map showing study area

Table 1 Average annual rainfall (mm) for Siran River basin and neighboring meteorological stations.

Months	Balakot	Haripur	Torghar	Muzaffarabad	Chilas	Naran	Abbottabad
January	64.11	73.65	63.70	103.47	48.69	60.00	64.10
February	123.00	104.14	94.60	198.54	80.90	89.00	123.00
March	124.60	124.46	71.60	206.56	90.97	104.00	124.60
April	114.90	104.14	74.40	132.02	108.26	84.00	114.60
May	62.10	73.66	52.30	73.13	145.61	46.00	62.10
June	88.40	76.20	47.50	57.20	111.71	43.00	88.40
July	167.70	246.38	93.50	186.91	122.35	124.00	167.70
August	162.90	243.84	100.50	161.36	89.64	163.00	162.90
September	98.40	96.52	61.30	56.56	55.05	57.00	98.40
October	38.00	50.80	31.80	35.83	50.95	24.00	38.00
November	35.00	30.48	14.30	46.62	35.63	20.00	35.00
December	47.90	48.26	24.70	76.18	87.74	15.00	47.90
Total Annual	1127.00	1272.54	730.20	1334.38	1027.49	829.00	1079
Average Annual	93.92	106.05	60.85	111.20	85.62	69.08	89.93

The overall accuracy was 72.78%, and Kappa coefficient was 0.70 or 70%. The task of C-factor values to each LULC class was created on existing literature (Ebabu et al., 2022; Wan et al., 2022). Typically, C-factor values range between 0 and 1, with higher values indicating greater surface protection through crop or vegetation coverage or various management techniques. It is essential to consider the accuracy of the LULC classifications and the reliability of the extracted values from the published literature. These factors are crucial to ensure that the computation of the C-factor is reliable and accurately reflects the conditions of each LULC class.

Support practice factor (P)

Support practice with the P-factor component in the RUSLE model assesses the efficiency and preservation of soil practices in mitigating soil loss. It is considered landscaping, contour farming, conservation

Table 2 R-factor scores for the Siran Basin and associated area under each class

Rainfall erosivity (R) classes and values	Area in km ²	Percent of total area
434.20–460.60	240.22	13.52
460.70–474.30	358.10	20.15
474.40–487.00	438.24	24.66
487.10–500.80	526.28	29.62
500.90–526.50	214.13	12.05
Total	1776.97	100.00

cultivation, and reducing soil erosion due to land management practices.

P-factor ranges from 0 to 1, where 1 value denotes fully implemented practices that efficiently prevent soil erosion, and 0 indicates the absence of such practices. The P-factor is determined based on the study region’s types and extent of preservation practices.

For example, terrace cultivation would have a higher P-factor than ineffective or poorly maintained practices. Calculating the P-factor in the RUSLE can involve various approaches depending on the specific preservation practices employed and data availability (Panagos, Borrelli, & Meusburger, 2015b). In the case of the Siran basin study, DEM was divided into five slope categories. Assuming the implementation

Table 3 Soil types and associated K-factor score for Siran Basin

Soil composition	Soil types		
	Lithosols (I)	Eutric Cambisols (be)	Glaciers
ms (sand) Topsoil	58.90	36.40	0.00
msilt (silt) Topsoil	16.20	37.20	0.00
mc (clay) Topsoil	24.90	26.40	0.00
orgC organic carbon	0.97	1.07	0.00
Fcsand	0.20	0.20	0.00
Fcl-si	0.76	0.85	0.00
Forge	0.93	0.91	0.00
Fhisand	0.99	1.00	0.00
K usle	0.14	0.15	0.00
K-value	0.02	0.02	0.00

Table 4 Soil types, composition (%), associated K-factor score, and area under each type for Siran Basin

Type	Sand	Silt	Clay	OC	K-factor	Area in km ²	Percentage
Lithosols	58.90	16.20	24.90	0.97	0.0184	242.48	13.65
Eutric Cambisols	36.40	37.20	26.40	1.07	0.0204	1534.5	86.35

of terrace agriculture in the basin, the required P-factor values for each slope class were determined from Koirala et al. (2019) and Shin (1999) studies. Subsequently, P-factor was computed for the study area using the technique specified by Shin (1999).

Results and discussion

Rainfall erosivity (R) factor

The regional distribution of rainfall and R-factor for the study area is illustrated in Figs. 3 and 4, respectively. The data presented in Table 1 were collected from the Regional Meteorological Office Peshawar

and other sources, covering the study region and surrounding areas from 2010 to 2020. Table 2 displays the predicted R-values for the Siran watershed and the corresponding areas within different classes. The investigation findings indicate that 58.33% of the study region falls within R-values 434.2–487. The eastern portion of the research region, which comprises 12.05% of the Siran watershed, exhibits the highest R-value while experiencing the lowest soil erosivity.

Soil erodibility (K) factor

The Siran basin has two main soil types: Eutric Cambisols (be) and Lithosols (I). Eutric Cambisols are the

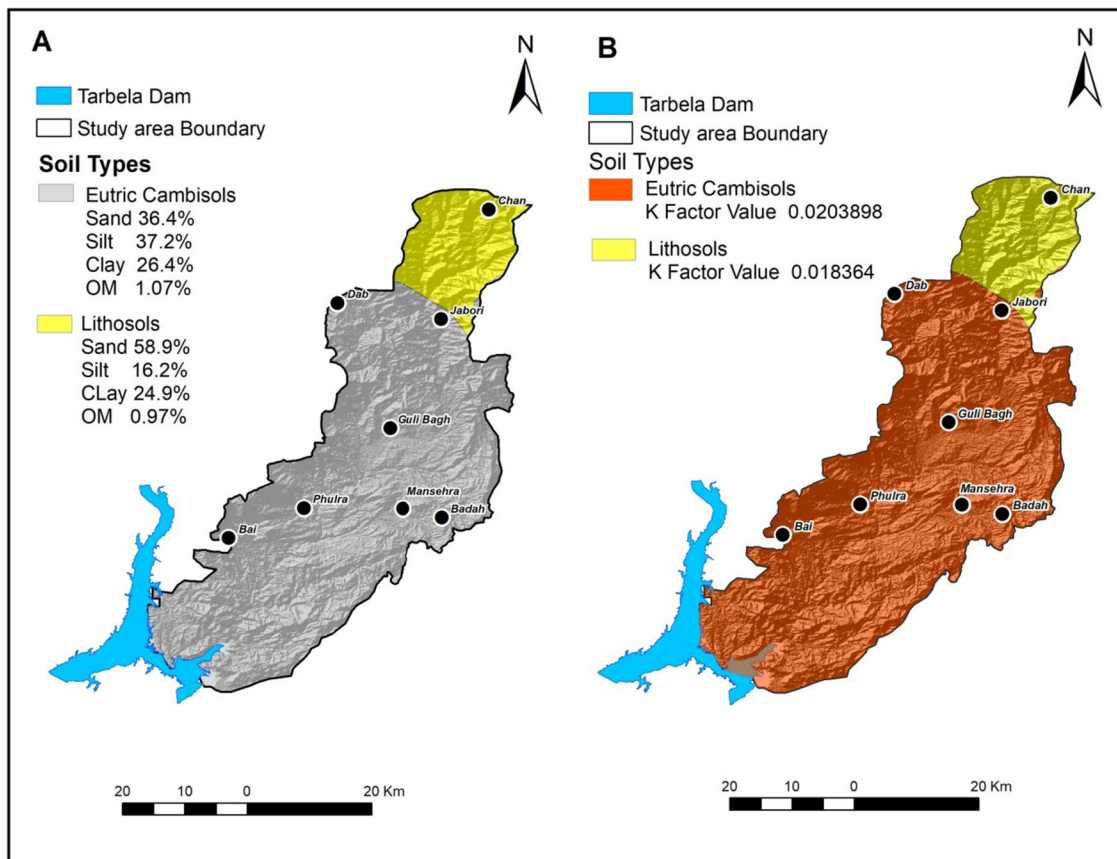


Fig. 5 A The spatial distribution of soil types. B Soil types and K-factor

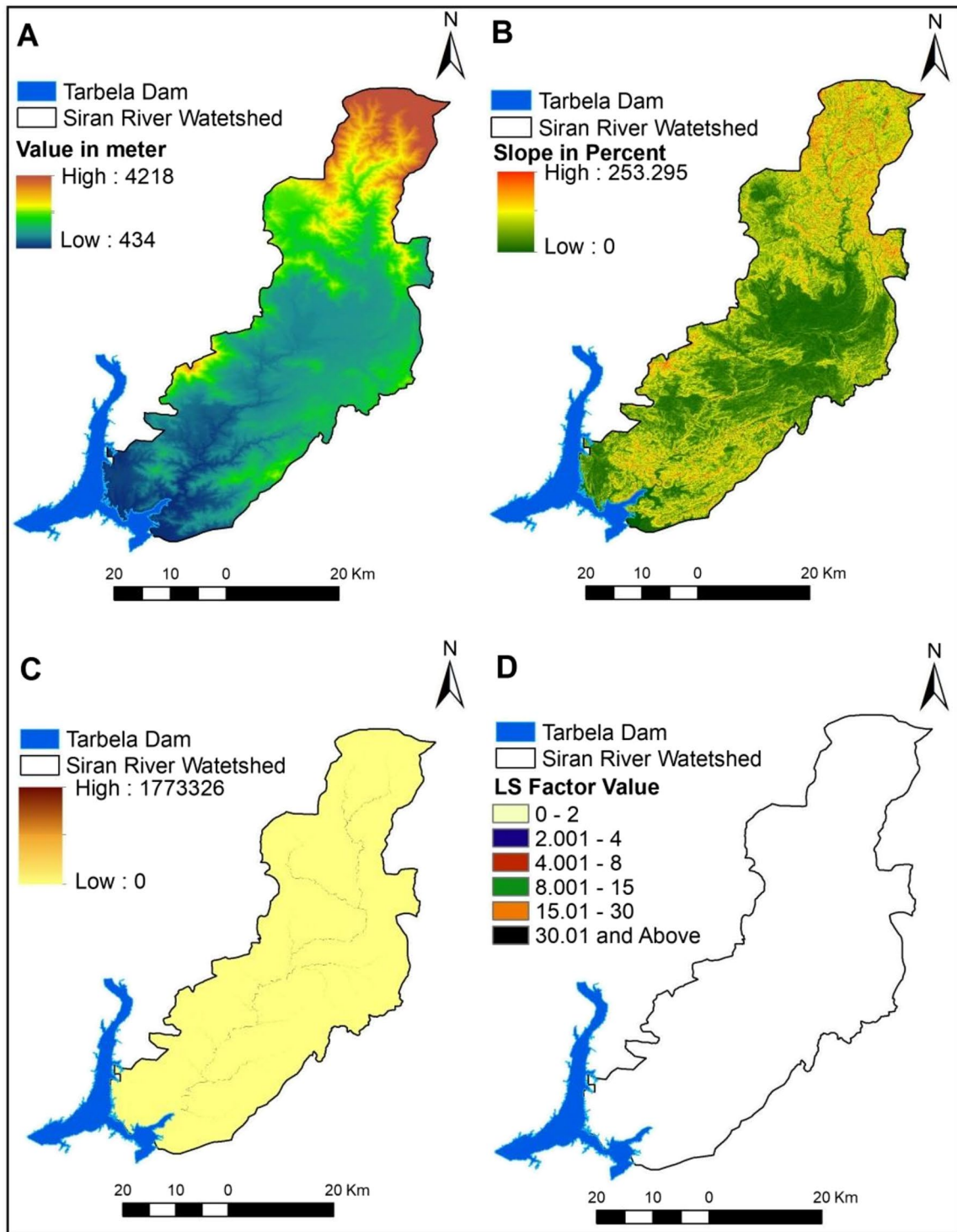


Fig. 6 **A** The DEM of Siran River watershed. **B** The slope in percentage. **C** The flow accumulation grid. **D** Spatial distribution of LS factor

Table 5 Siran Basin LS-factor scores and associated area under each class

LS factor value	Area in km ²	Percentage of total area
0–2	1694.791	95.890
2.1–4	40.610	2.290
4.1–8	17.871	1.010
8.1–15	7.130	0.400
15.1–30	3.392	0.190
>30	3.850	0.220
	1767.97	100

predominant soil type, covering 86.36% of the total area. These soils are highly fertile and widely recognized as ideal for agriculture. They exhibit a loam texture, roughly equal amount of sand, silt, and clay. The A-horizon of Eutric Cambisols is typically yellowish-brown, although it can occasionally be a vivid red. The best Cambisols are found on rocky terrain with tree cover.

On the other hand, Lithosols are thin soils with poorly developed horizons. They form either in mountainous regions or due to the resistance of underlying parent rocks to weathering. Lithosols are commonly found on rocky slopes where deep soil development is hindered by erosion caused by rainfall. Vegetation cover in Lithosols is minimal, mainly comprising shrubs or grasses. These soils are unsuitable for farming due to their shallow depth, steep slopes, and high susceptibility to erosion. In the Siran watershed, Lithosols account for 13.65% of the area. Tables 3 and 4 provide information on the soil types, texture, K-value, and respective areas.

Figure 5A illustrates that soils dominate the soil types in the study area, covering a substantial portion

of the study area. In contrast, Lithosols are found in smaller patches, primarily sited in the upper stream region of the Siran River basin. As shown in Fig. 5B, most of the research region exhibits a low K-factor score of 0.0204, indicating a low susceptibility to soil erosion. However, despite occupying only 13.65% of the total areas, the highest K-factor value in lithosols exhibit is 0.0184%. The higher concentration of sand in the lithosols soil can be attributed to its elevated value. Soils with a higher sand content are extremely vulnerable to erosion compared to those with higher clay or organic matter content. The reduced binding ability of sands makes them easily transported by water or wind. Thus, the higher sand content in this area's Lithosols soil may contribute to the observed elevated soil erodibility factor values.

Slope length and steepness factor (LS)

LS factor is crucial in assessing potential for soil loss as it considers flow concentration, slope length, and gradient. Fig. 6A visualizes the DEM, while Fig. 6B displays the slope in percentage within the research region. Figure 6C, D depicts the flow accumulation grid and the geographical distribution of LS factor across the research area. The data presented in Table 5 are the values of the LS factor for the Siran watershed ranging from 0.1 to 1439. A significant portion of the area (95.89%) exhibits an LS factor ranging from 0.1 to 2. However, a higher LS factor range of 30.1–1439 is concentrated in a small area of 3.87 km² (0.22%), primarily associated with steep terrain along streams and rivers. The analysis reveals that vertical slopes are predominantly located in the northeastern region of the study area, indicating a greater likelihood of soil loss in these specific locations

Table 6 Siran Basin, LULC classes, associated C-factor scores, and area under each class

Land use land cover classes	C value	Area in km ²	Percentage	Reference
Barren land	1.000	116.440	6.590	Hurni (1985)
Rangeland	0.050	783.690	44.330	Tiruneh and Ayalew (2015)
Cropland	0.150	131.570	7.440	Wischmeier and Smith (1978)
Built-up area	0.004	281.240	15.910	Kayet et al. (2018)
Natural vegetation	0.010	416.120	23.540	Tiruneh and Ayalew (2015)
Snow and ice	0.000	12.500	0.710	Kayet et al. (2018)
Water bodies	0.000	26.400	1.490	Erdogan et al. (2006)
Total		1767.96	100	

Table 7 Showing C-factor values, area in km², and percentage of Siran River.

S. no	C-factor values	Area in km ²	Percentage
1	0–0.00784	740.280	41.830
2	0.00785–0.0471	783.880	44.300
3	0.0472–0.049	131.590	7.440
4	0.015–1	113.900	6.440
Total		1769.65	100.00

Land cover and management factor (C)

Table 6 provides a comprehensive overview of the LULC categories identified in the research region, the percentage of each class, and their corresponding values of the C-factor. The C-factor is a decisive component of the RUSLE equation with the influence of

vegetation and management practices on soil loss. It is typically scaled from 0 to 1, with 0 indicating minimal erosion potential and 1 suggesting a higher likelihood of erosion. Most of the study region, comprising over 80%, comprises agricultural and barren land. These land types generally exhibit higher C-factor values, indicating increased susceptibility to soil loss.

In contrast, forested areas display lower C-factor values, indicating a reduced risk of soil erosion. Table 7 and Fig. 7 further provide detailed information on the extent of each C-factor class, which ranges from very low to very high erosion potential. Notably, only a small portion (0.16%) of the research area, considered for 62.34% of the total size, is classified as having an exceptionally high risk of soil loss. While specific locations within the research region present a significant erosion risk, the remaining areas generally demonstrate a moderate to high erosion potential.

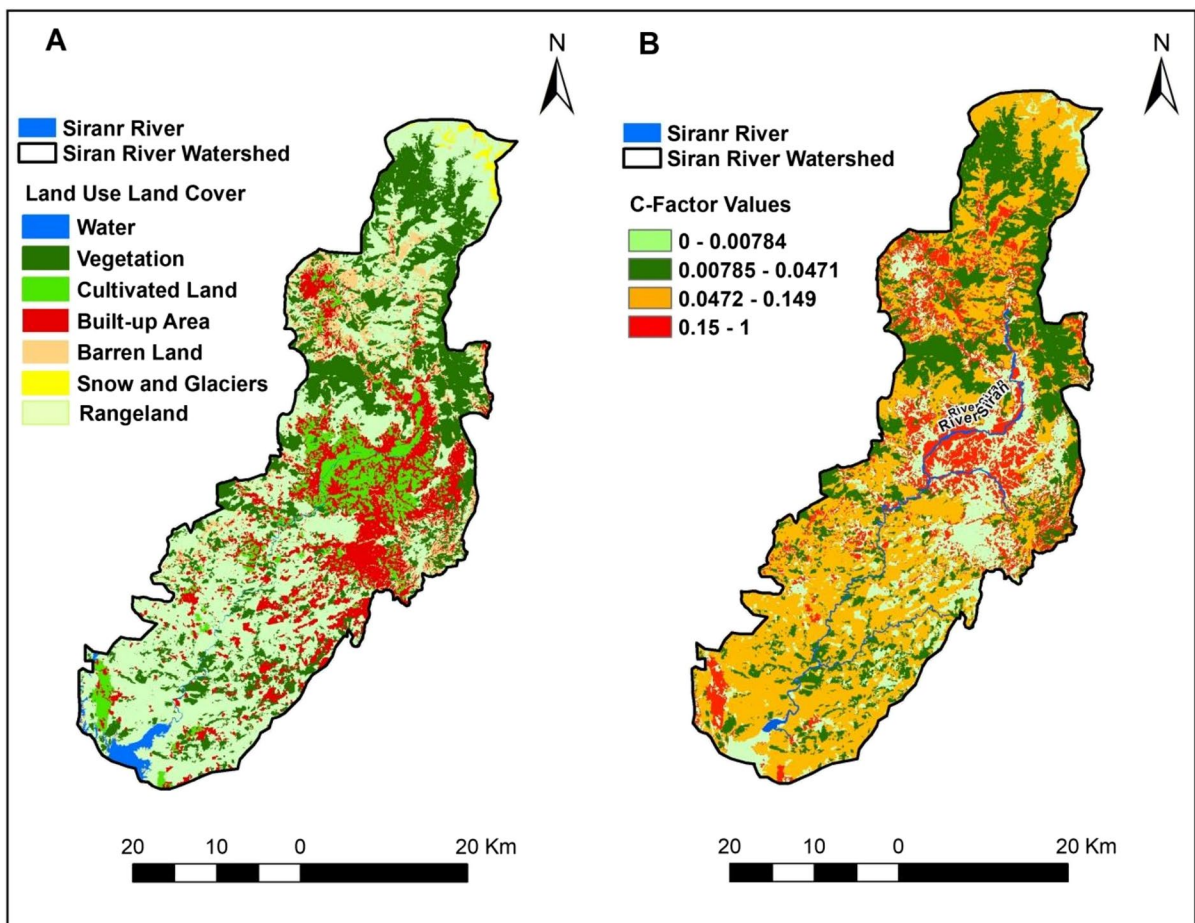


Fig. 7 A The LULC of Siran River watershed. B Spatial distribution of C-factor values

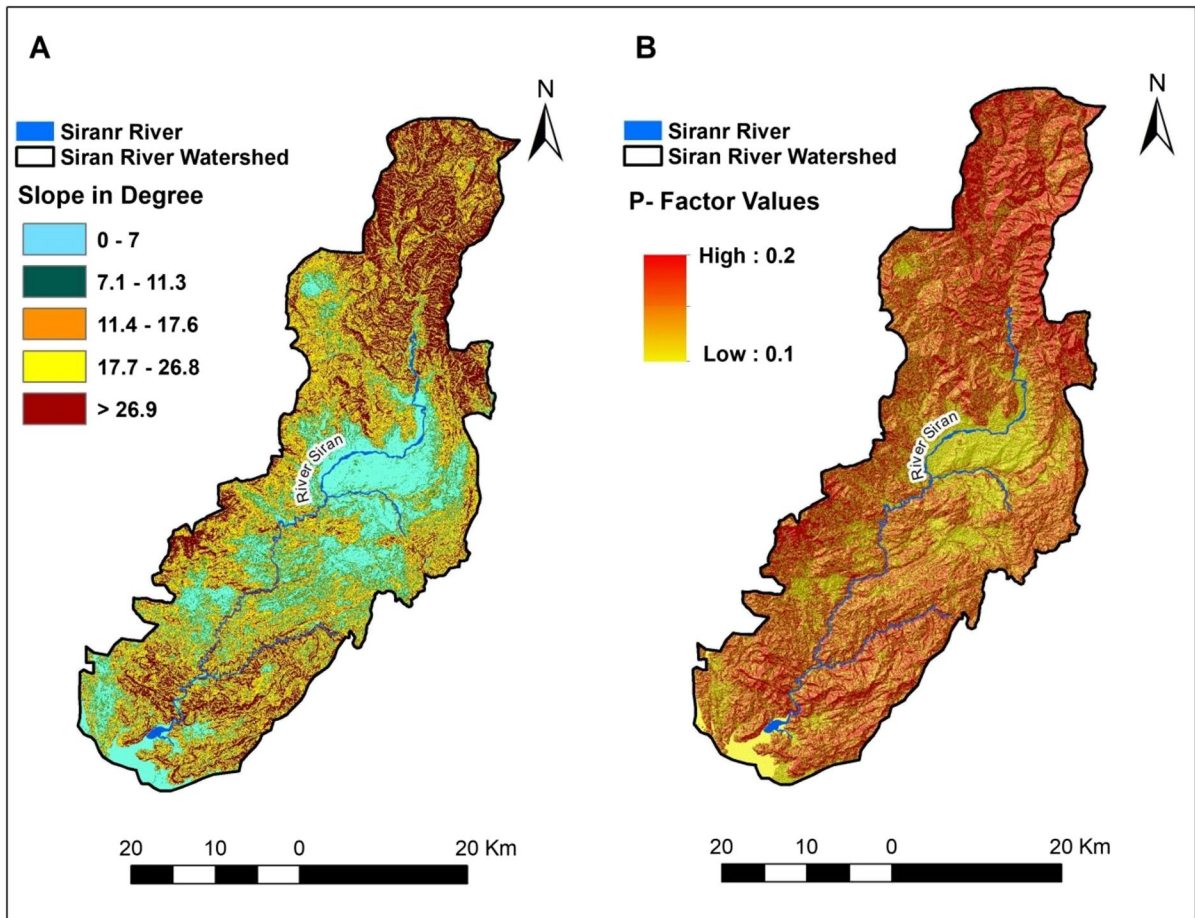


Fig. 8 **A** The spatial distributions of slope classes (slope in degree) for the Siran River watershed. **B** The spatial distributions of support practice (P-factor) values for the Siran River watershed

Support practice factor (P)

Shin (1999) and Koirala et al. (2019) highlighted the P-factor, which characterizes essential acts in assessing the soil erosion risk by considering the effectiveness of support practices in mitigating erosion. The values of the P-factor are visualized in the study.

Figure 8A, B depicts the slope in degrees and the geographical representation of the P-factor value, respectively. These visualizations offer insights into the steepness of slopes and spatial variation in reducing soil erosion to check the effectiveness of support practices. Table 8 shows slope classes, their respective areas, and the corresponding P-factor scores. The

Table 8 Siran basin slope classes, area, and associated P-factor scores of each class

S. no	Slope categories percent slope	Support practice	P-factor value	Area in km ²	% of basin area
1	0 – 7	Terrace farming	0.100	392.85	22.20
2	7.1 – 11.3		0.120	225.48	12.75
3	11.4 – 17.6		0.160	286.67	16.19
4	17.7 – 26.8		0.180	402.18	22.72
5	>26.9		0.200	462.46	26.14
Total				1769.64	100.00

P-factor score ranges from 0 to 1, where 0 represents highly effective support practices that resist erosion, while 1 indicates lower resilience to erosion.

Annual soil loss

The study’s key findings are summarized in Table 9 and Figs. 9–12. This research reveals an average annual soil loss of 0.154 million tons, equal to 0.871 tons per hectare or 0.871 tons per hectare. The study region is based on soil erosion intensity and is classified into five classes, i.e., very high, high, moderate, low, and very low. Our analysis demonstrates that a significant portion of the research area has very low soil erosion, which is 72.94% with a rate of 0.021 tons

per hectare per year, contributing to the total annual soil loss is 1.67% only. Areas characterized by low to moderate soil erosion rates of 0.021–0.5 tons/ha/year and 0.51–1 tons/ha/year account for approximately 15% of overall annual soil loss, occupying 24.67% of the Siran basin.

In contrast, regions exhibiting extremely high soil erosion rates (over 10 tons per hectare per year) are found in only 0.15% of the total area, yet they donate to 75.76% of total yearly soil loss. These areas are often located on rocky terrain near streams and rivers, with high LS and C-factors indicating poor crop management practices. The study highlights the critical role of actual erosion control measures in this highly susceptible area to mitigate and preserve soil

Table 9 Showing percentages and erosion severity of Siran River

Soil loss intensity		Area in km ²	Area in Ha	% of total area	Soil loss tons/ha/year	% of total loss
Qualitative	Quantitative					
Very low erosion	0–0.02	1290.71	129,071.0	72.94	2581.42	1.67
Low erosion	0.021–0.5	436.62	43,661.80	24.67	21,830.90	14.15
Moderate erosion	0.51–1	21.51	2151.27	1.22	2151.27	1.39
High erosion	1.1–10	18.04	1804.32	1.02	10,825.92	7.02
Very high erosion	10.1–840	2.72	271.72	0.15	116,839.60	75.76
Total		1769.69	176,969.4	100	154,229.11	100
Siran River average annual total soil loss million tons/year and annual soil loss per tons/ha/year.				0.154		
				0.871		

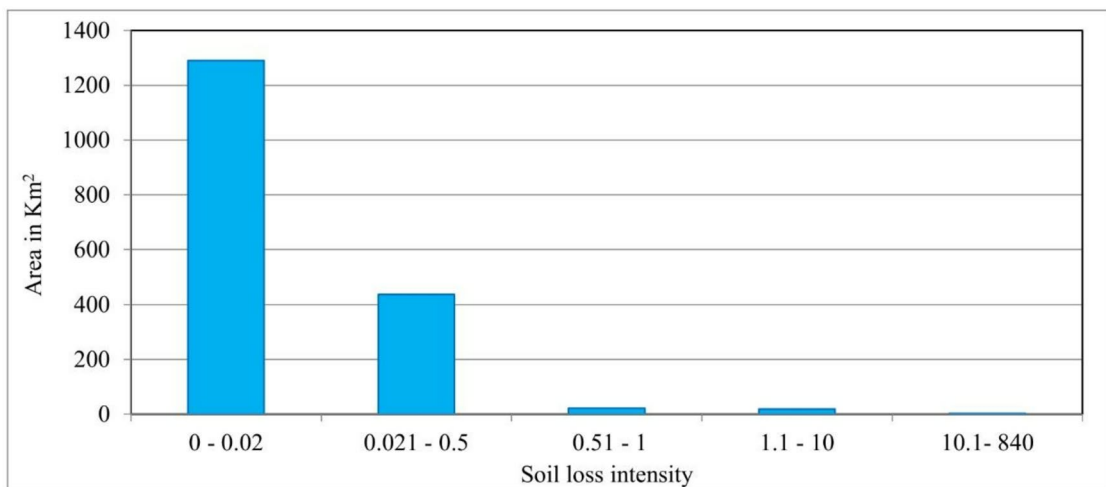


Fig. 9 Siran River watershed, soil loss intensity, and area in km²

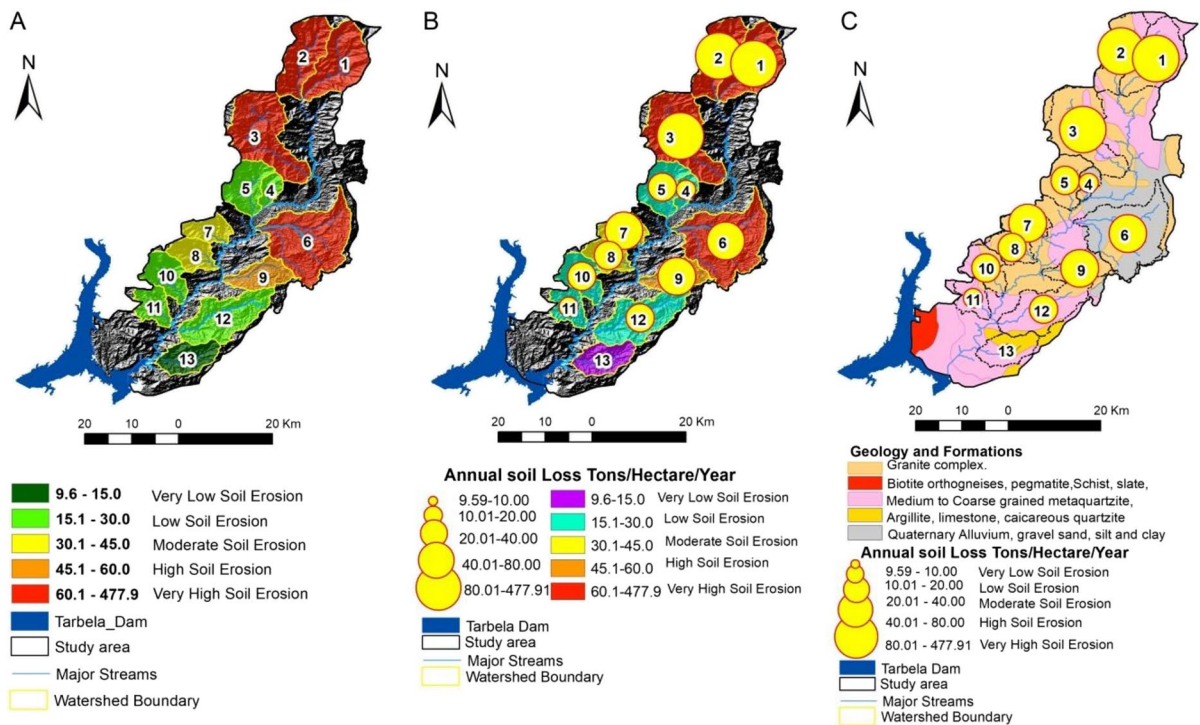


Fig. 10 **A** Watershed level annual soil loss. **B** Sub-watershed level of Siran River annual soil loss tons/ha/year. **C** Sub-watershed level and annual soil loss tons/ha/y vs. geology

loss health. Our research findings reveal the significant issue of soil erosion in Siran Basin, particularly the areas characterized by limited vegetation cover and steep slopes. To address this problem and ensure sustainable land use, the study provides valuable insights for implementing effective soil conservation and management strategies. Notably, areas identified as soil erosion hotspots exhibit high erosion rates due to sparse forest cover, shallow sandy or gravelly soils, improper agricultural practices, and the absence of soil conservation measures. These identified areas demonstrate medium to high soil erodibility, indicating their susceptibility to erosion.

Additionally, heavy rainfall contributes to the basin area, with approximately 26.14% of the total area exhibiting slopes exceeding 26.9% and corresponding P scores of 0.2. Based on these findings, it is crucial to prioritize implementing targeted soil preservation and management measures in these vulnerable areas. This will help mitigate soil erosion, promote sustainable land use practices, and safeguard the long-term health and productivity of the Siran Basin's soil

resources. Most erosion hotspots in the Siran River basin are concentrated in the northern regions. This spatial distribution is depicted in Fig. 9, which showcases the area in km^2 and the intensity of soil loss. Additionally, Fig. 10A, B presents soil loss annually at the watershed level, while Fig. 10C highlights the association between geology and annual soil loss.

Various parameters were considered to assess the annual soil loss by using RUSLE model as illustrated in Fig. 11A–E. This figure depicts the factors utilized in the annual soil loss calculation. Furthermore, Fig. 11F provides the geographical distribution of erosion-prone locations, commonly referred to as erosion hotspots, within the Siran River watershed. Tables 9 and 10 and Fig. 11A, B present the Siran River basin annual soil loss at the sub-watershed level. Our analysis shows that sub-watersheds 1, 2, and 3 have rates of 207.30, 166.23, and 477.91 tons/ha/year annual loss, respectively. These sub-watersheds predominantly consist of granite as their underlying geology.

Granite undergoes chemical weathering through hydrolysis of its feldspar component, forming weathered

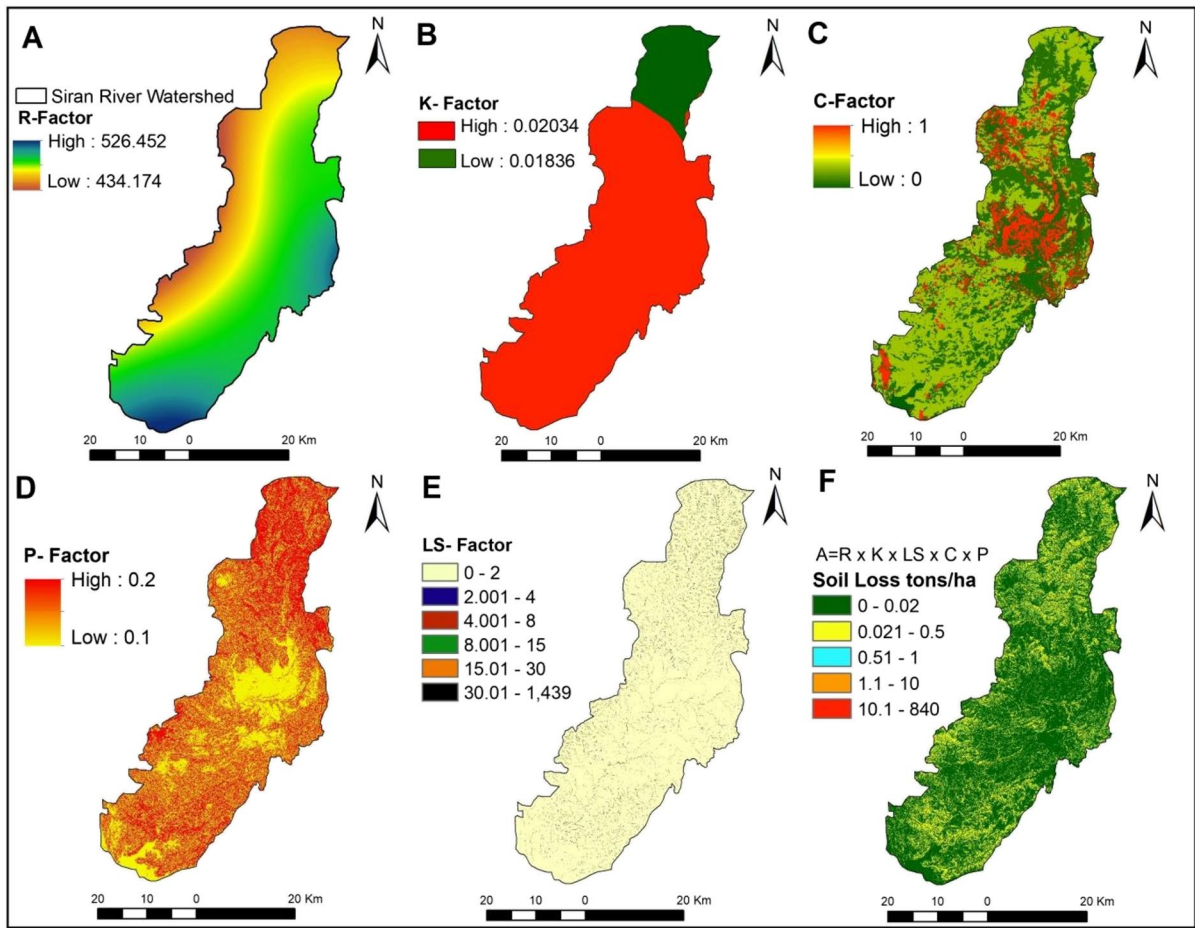


Fig. 11 A R-factor. B K-factor. C C-factor. D P-factor. E LS-factor. F Annual soil loss and erosion hotspot areas ($R \times K \times LS \times C \times P$)

material known as Grus (Chung et al., 2020). Granite also undergoes chemical weathering even under icy conditions, known as polar weathering. Moreover, urban areas such as Mansehra City, Attar Sheesha, Chitta Batta, etc., primarily contribute to WS-6, which exhibits a very high soil erosion rate. The surrounding area of WS-6 is covered by Quaternary sediments, which consist of loose deposits of gravel, sand, silt, and clay. These quaternary deposits are composed of loose, unconsolidated rock that is highly susceptible to erosion.

Different studies have been carried out in various Pakistan regions to estimate the annual soil loss using the RUSLE model. Ullah et al. (2018) presented a study on the district Chakwal, which revealed a yearly soil loss of 97.81 m tons ha⁻¹ year⁻¹, averaging 70 to 230 tons/ha/year. Maqsoom et al. (2020) focused

on the Chitral River and estimated 58 tons/ha/year mean yearly soil loss. In the Ghabbir basin, Ashraf et al. (2017) found average annual soil loss is 22 tons/hectare/year. Butt et al. (2011) investigated the Simly basin in the Margalla hills and reported an average yearly soil loss of 14 tons/ha/year.

According to Batool et al. (2021), the Potohar basin experiences recorded 325.39 tons/ha annual soil loss. Gilani et al. (2021) conducted a study on soil erosion in the KP province of Pakistan and estimated yearly soil loss of 11.78 and 21.97 tons/ha/year. Zaidi and Khan (2018) conducted a study on the Kunhar River and found an average soil loss of 21.18 tons/ha/year. In the present study, the average soil loss was calculated to be 0.871 tons/hectare/year, with a total yearly soil loss of 0.154 million tons in

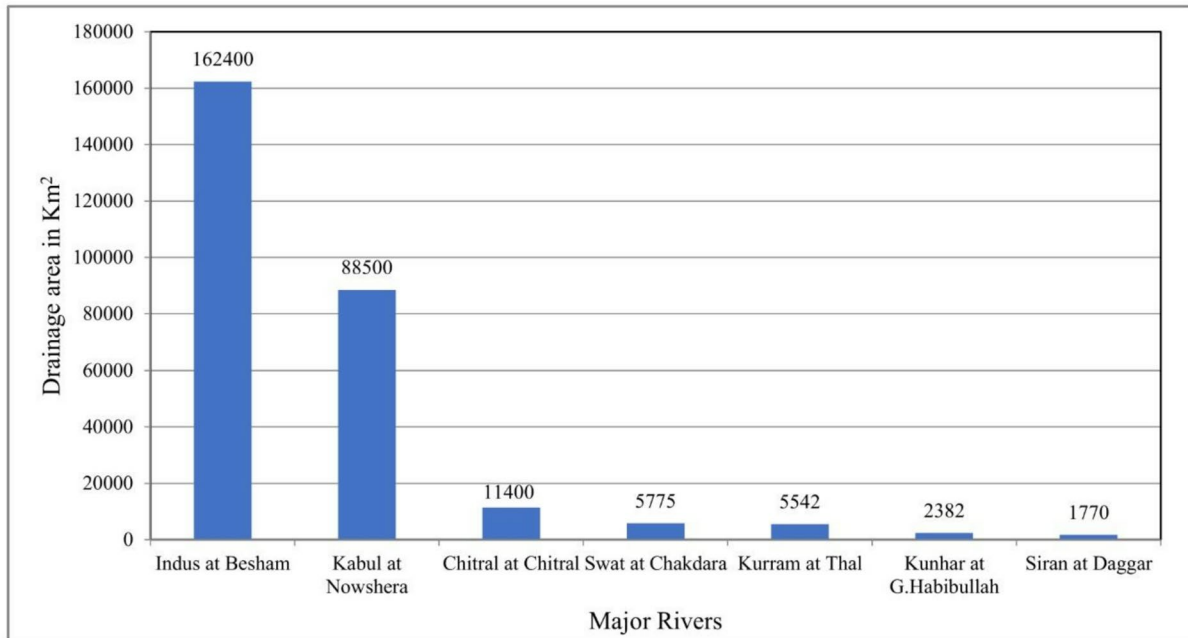


Fig. 12 Major rivers of KP and their assessment with Siran River

the Siran River watershed. Table 11 shows Gilani et al. (2021)'s projections of annual soil loss for Pakistan and its seven administrative regions. The analysis reveals that the estimates of annual soil loss obtained in the current research are significantly lower than other predictions. This difference could be attributed to the relatively unexplored and lush green nature of

the Siran Valley, in contrast to the Kunhar and Chitral River watersheds.

Results comparison and validation

Moreover, regarding water discharge, the Siran River is relatively smaller than other local rivers. Figure 12

Table 10 Sub-watershed of Siran River and annual soil loss tons/ha/year

Sub watershed	Important settlements	Annual soil loss t/ha/yr	Soil erosion intensity t/ha/yr
WS-1	Jabori, Managucha	207.30	Very high soil erosion
WS-2	Jabber, Mundi, Devoli	166.23	Very high soil erosion
WS-3	Icherrian, Batta, Khakoo, Harorri	477.91	Very high soil erosion
WS-4	Guli Bahg, Tangri	17.72	Low soil erosion
WS-5	Chirikikot, Bada Bagh, Shinnai	25.56	Low soil erosion
WS-6	Jabba atta Sheesha, Chitta batta, Manshera	63.19	High soil erosion
WS-7	Parehna, Thaker Mera, Thathi	41.19	Moderate soil erosion
WS-8	Devi, Phulra, Kandar	32.58	Moderate soil erosion
WS-9	Narian, Ogra	46.31	High soil erosion
WS-10	Dara Mohan, Bai Bohal Mohar Kalan	28.69	Low soil erosion
WS-11	Danseri, Dan Seri, Sunyara	15.13	Low soil erosion
WS-12	Sherwan, Khapir, Shaheenabad	23.12	Low soil erosion
WS-13	Kakotri, Jarial sheriff, Gul bandi	9.59	Very low soil erosion

Table 11 Siran River and average soil loss of various regions of Pakistan

S. no	Area/watershed	Soil loss tons/ha/year	Annual Soil loss tons/ha/year	Reference
1	Potohar Region Pakistan	148	325.39	Batool et al. (2021)
2	Chakwal (Punjab)	70–230	97.81	Ullah et al. (2018)
3	Chitral River basin	58		Maqsoom et al. (2020)
4	Ghabbir Watershed of Photohar Plateau	22		Ashraf et al. (2017)
5	Simly watershed of Margella Hill	14		Butt et al. (2011)
6	Kunhar River Watershed	21.18	5.1 million tons	Zaidi and Khan (2018)
7	Siran River Watershed	0.871	0.154 million tons	Current study

provides an overview of the basin areas of significant rivers within the Khyber Pakhtunkhwa province, illustrating the relative size of the Siran River. The environmental conditions in the Kunhar and Siran watersheds exhibit considerable similarities and flow in roughly parallel directions. However, unlike the Kunhar basin, the Siran River basin remains largely unexplored. Nevertheless, the growing number of tourists has rapidly expanded motels and lodges in the Naran region. It is estimated that Naran alone has approximately 1500 hotels of varying sizes. These human activities contribute to sediment production, eventually transported downstream by the Kunhar River.

Conclusions

The primary objective of this research was to count the Siran River basin’s annual soil loss using the integration of RUSLE, GIS, and RS techniques. The study finding reveals that a small portion of the Siran River basin, particularly the northern part, has experienced significant soil loss, while the major portion of the basin has low to moderate levels of soil loss. The annual soil loss estimated in the basin is 0.154 million tons, equal to 0.871 tons per year per hectare. The spatial distribution analysis identifies specific areas in the far north of the basin as erosion hotspots, indicating a higher susceptibility to soil erosion as linked to the southern part. This form of soil erosion is relevant to the challenges faced by less economically developed countries, where soil erosion is a significant problem. For instance, over 30 to 32.80 million of land in India is under river erosion. Similarly, in Iran, soil loss occurs at a rate of 24 tons per acre annually. In Pakistan, soil erosion affects over 16

million hectares, accounting for approximately 20% of the country’s total geographic area. Of this total, 11.2 million hectares are at risk of water erosion.

On a global scale, approximately 20 billion tons of sediments are produced annually, with more than 80% of this sediment ultimately reaching the world’s oceans. The remaining 20% is deposited in reservoirs and dams. These figures highlight the widespread and significant impact of soil erosion worldwide. Agriculture plays a vital role in Pakistan’s economy, with a significant portion of agricultural output relying on the country’s abundant water resources, 50% of which is derived from surface water. The effective utilization of these water resources is closely linked to the management of surface waters. One of Pakistan’s most important water storage facilities is the Tarbela Dam, constructed on the Indus River. Over time, the dam has faced challenges due to soil erosion and changes in the surrounding region’s LULC dynamics. The continuous accumulation of sediment within the dam has led to a reduction in its water storage capacity.

Tarbela Dam, the largest earth-filled reservoir in Pakistan, serves dual purposes of hydroelectricity generation and irrigation. According to Wallingford (1998), the average annual sediment influx into the dam is approximately 81,000 million cubic meters (mm³), with varying annual influxes of fine sediment ranging from 100 to 300 metric tons (MT) between 1967 and 1996. Pakistan Water and Power Development Authority (WAPDA) predicts that the Tarbela Dam will continue to lose water storage capacity, having already experienced a significant decline. Neglecting this issue over an extended period could lead to a major catastrophe. Sedimentation is essential in influencing the reservoir’s storage capacity, emphasizing the importance of accurately assessing sediment inflow into the reservoir.

The findings of this study are expected to provide valuable understanding for governments and relevant organizations in making informed decisions to mitigate soil loss and address the sedimentation issue. Addressing these challenges aims to ensure the long-lasting sustainability of water resources and optimize the functioning of critical infrastructure such as the Tarbela Dam.

Acknowledgements The authors acknowledge the Department of Geography, University of Peshawar, Department of Geography Islamia College Peshawar, and Department of Petroleum and Mining Engineering, Tishk International University, Erbil, Iraq.

Author contribution Mehwish Mehwish: original draft writing, formal analysis, investigation, and methodology; Muhammad Jamal Nasir; Supervision, writing review, and editing; Abdur Raziq; rewriting some parts, correcting of English, and reviewing the manuscript. Ayad M. Fadhil Al- Quriashi; extensive reviewing, editing and finalizing original draft and Fadhil Ali Ghaib; review manuscript.

Data availability The data used in this study are available on request from the corresponding author.

Declarations

Ethics approval All authors have read, understood, and have complied as applicable with the statement on “Ethical responsibilities of Authors” as found in the Instructions for Authors and are aware that with minor exceptions, no changes can be made to authorship once the paper is submitted.

Conflict of interest The authors confirm no conflict of interest.

References

- Ahmad, M., Jadoon, M. A., Ahmad, I., & Khan, H. (2007). Impact of trainings imparted to enhance agricultural production in district Mansehra. *Sarhad Journal of Agriculture*, 23(4), 1211.
- Angulo-Martínez, M., & Beguería, S. (2009). Estimating rainfall erosivity from daily precipitation records: A comparison among methods using data from the Ebro Basin (NE Spain). *Journal of Hydrology*, 379, 111–121. <https://doi.org/10.1016/j.jhydrol.2009.09.051>
- Akça, E., Büyüç, G., İnan, M., & Kırpık, M. (2022). Sustainable management of land degradation through legume-based cropping system. In *Advances in legumes for sustainable intensification* (pp. 267–280). Academic Press. <https://doi.org/10.1016/B978-0-323-85797-0.00029-X>
- Arabameri, A., Pradhan, B., Pourghasemi, H. R., & Rezaei, K. (2018). Identification of erosion-prone areas using different multi-criteria decision-making techniques and GIS. *Geomatics, Natural Hazards and Risk*, 9, 1129–1155. <https://doi.org/10.1080/19475705.2018.1513084>
- Arif, A. M., Hameed, A., & Anwar, A. (2022). *Problems faced by visitors in Pakistan: A case study of Kaghan Valley, Mansehra* (pp. 74–82). Global Political Review, VII(1). [https://doi.org/10.31703/gpr.2022\(VII-I\).08](https://doi.org/10.31703/gpr.2022(VII-I).08)
- Ashraf, A., Abuzar, M. K., Ahmad, B., Ahmad, M. M., & Hussain, Q. (2017). Modeling risk of soil erosion in high and medium rainfall zones of Pothwar Region, Pakistan: Assessment of soil erosion risk. Proceedings of the Pakistan Academy of Sciences: B. *Life and Environmental Sciences*, 54, 67–77.
- Aslam, B., Maqsoom, A., Alaloul, W. S., Musarat, M. A., Jabbar, T., & Zafar, A. (2021). Soil erosion susceptibility mapping using a GIS-based multi-criteria decision approach: Case of district Chitral, Pakistan. *Ain Shams Engineering Journal*, 12, 1637–1649. <https://doi.org/10.1016/j.asej.2020.09.015>
- Awan, R. S., Khan, A., Liu, C., Yang, S., Zang, Q., Wu, Y., & Ali, S. (2021). Subsurface geological model of sedimentary and metasedimentary wedge from Mansehra to Battal based on gravity data, Hazara area, Pakistan. *Energy Geoscience*, 2, 229–237. <https://doi.org/10.1016/j.engeos.2021.06.004>
- Bag, R., Mondal, I., Dehbozorgi, M., Bank SP, Das, D. N., Bandyopadhyay, J., Pham, Q. B., Al-Quraishi, A. M. F., & Nguyen, X. C. (2022). Modelling and mapping of soil erosion susceptibility using machine learning in a tropical hot sub-humid environment. *Journal of Cleaner Production*, 364, 132428. <https://doi.org/10.1016/j.jclepro.2022.132428>
- Batool, S., Shirazi, S. A., & Mahmood, S. A. (2021). Appraisal of soil erosion through RUSLE model and hypsometry in Chakwal Watershed (Potwar-Pakistan). *Sarhad Journal of Agriculture*, 37, 594–606. <https://doi.org/10.17582/journal.sja/2021/37.2.594.606>
- Biswas, S. S., & Pani, P. (2015). Estimation of soil erosion using RUSLE and GIS techniques: A case study of Barakar River basin, Jharkhand, India. *Modeling Earth Systems and Environment*, 1, 1–13. <https://doi.org/10.1007/s40808-015-0040-3>
- Butt, M. J., Mahmood, R., & Waqas, A. (2011). Sediments deposition due to soil erosion in the watershed region of Mangla Dam. *Environmental Monitoring and Assessment*, 181, 419–429. <https://doi.org/10.1007/s10661-010-1838-0>
- Cardoso, D. P., Silva, E. M., Avanzi, J. C., Muniz, J. A., Ferreira, D. F., Silva, M. L. N., & Curi, N. (2020). Rainfall erosivity factor: An R package for rainfall erosivity (R-factor) determination. *Catena*, 189, 104509. <https://doi.org/10.1016/j.catena.2020.104509>
- Chauhan, N., Kumar, V., Paliwal, R., & Kakkar, R. (2020). Quantifying the risks of soil erosion using Revised Universal Soil Loss Equation (RUSLE) and GIS technology for Ghaggar River Basin—A case of Lower Shivaliks. *Mukt Shabd Journal*, 9, 221–232.
- Chen, Y., Duan, X., Zhang, G., Ding, M., & Lu, S. (2022). Rainfall erosivity estimation over the Tibetan plateau based on high spatial-temporal resolution rainfall records. *International Soil and Water Conservation Research*, 10, 422–432. <https://doi.org/10.1016/j.iswcr.2022.01.004>
- Cherif, K., Yahia, N., Bilal, B., & Bilal, B. (2023). Erosion potential model-based ANN-MLP for the spatiotemporal modeling of soil erosion in wadi Saida watershed. *Modeling Earth Systems and Environment*, 1–23. <https://doi.org/10.1007/s40808-022-01657-3>

- Chuenchum, P., Xu, M., & Tang, W. (2020). Predicted trends of soil erosion and sediment yield from future land use and climate change scenarios in the Lancang–Mekong River by using the modified RUSLE model. *International Soil and Water Conservation Research*, 8, 213–227. <https://doi.org/10.1016/j.iswcr.2020.06.006>
- Chung, H. Y., Jung, J., Lee, D. H., Kim, S., Lee, M. K., Lee, J. I., & Kim, K. (2020). Chemical weathering of granite in ice and its implication for weathering in polar regions. *Minerals*, 10, 185. <https://doi.org/10.3390/min10020185>
- Das BM (2021) *Principles of geotechnical engineering*. Cengage Learning.
- Ebabu, K., Tsunekawa, A., Haregeweyn, N., Tsubo, M., Adgo, E., Fenta, A. A., & Poesen, J. (2022). Global analysis of cover management and support practice factors that control soil erosion and conservation. *International Soil and Water Conservation Research*, 10, 161–176. <https://doi.org/10.1016/j.iswcr.2021.12.002>
- Eckstein, D., Künzel, V., Schäfer, L., & Wings, M. (2019). Global climate risk index 2020 (pp. 1–50). Germanwatch, Bonn, Germany.
- Egbueri, J. C., Igwe, O., & Ifediegwu, S. I. (2022). Erosion risk mapping of Anambra State in southeastern Nigeria: Soil loss estimation by RUSLE model and geoinformatics. *Bulletin of Engineering Geology and the Environment*, 81, 91. <https://doi.org/10.1007/s10064-022-02589-z>
- Erdogan, H. E., Erpul, G., & Bayramin, I. (2006). *Use of USLE/GIS methodology for predicting soil loss in a semi-arid agricultural watershed*. Department of Soil Science, University of Ankara.
- Erenstein, O. C. (1999). *The economics of soil conservation in developing countries: The case of crop residue mulching*. Wageningen University and Research.
- Fadhil, A. M. (2013). Sand dunes monitoring using remote sensing and GIS techniques for some sites in Iraq. In *PIA-GENG 2013: Intelligent information, control, and communication technology for agricultural engineering* (pp. 28–36) (p. SPIE). <https://doi.org/10.1117/12.2019735>
- Gayen, A., Saha, S., & Pourghasemi, H. R. (2020). Soil erosion assessment using RUSLE model and its validation by FR probability model. *Geocarto International*, 35, 1750–1768. <https://doi.org/10.1080/10106049.2019.1581272>
- Gelagay, H. S., & Minale, A. S. (2016). Soil loss estimation using GIS and remote sensing techniques: A case of Koga watershed, Northwestern Ethiopia. *International Soil and Water Conservation Research*, 4, 126–136. <https://doi.org/10.1016/j.iswcr.2016.01.002>
- Ghosal, K., & Das, B. S. (2020). A review of RUSLE model. *Journal of the Indian Society of Remote Sensing*, 48, 689–707. <https://doi.org/10.1007/s12524-019-01097-0>
- Gilani, H., Ahmad, A., Younes, I., & Abbas, S. (2021). *Estimation of annual soil erosion dynamics (2005–2015) in Pakistan using Revised Universal Soil Loss Equation (RUSLE)*. Authorea Preprints. <https://doi.org/10.22541/au.160946369.92099648/v1>
- Gilani, H., Ahmad, A., Younes, I., & Abbas, S. (2022). Impact assessment of land cover and land use changes on soil erosion changes (2005–2015) in Pakistan. *Land Degradation and Development*, 33, 204–217. <https://doi.org/10.1002/ldr.4138>
- Habtu, W., & Jayappa, K. S. (2022). Assessment of soil erosion extent using RUSLE model integrated with GIS and RS: The case of Megech-Dirma watershed, Northwest Ethiopia. *Environ Monit Assess*, 194, 318. <https://doi.org/10.1007/s10661-022-09965-y>
- Hossini, H., Karimi, H., Mustafa, Y. T., & Al-Quraishi, A. M. F. (2022). Role of effective factors on soil erosion and land degradation: A review. *Environmental Degradation in Asia: Land Degradation, Environmental Contamination, and Human Activities*, 221–235. https://doi.org/10.1007/978-3-031-12112-8_11
- Hurni, H. (1985). *Soil conservation manual for Ethiopia*. Ministry of Agriculture.
- Hoyos, N. (2005). Spatial modeling of soil erosion potential in a tropical watershed of the Colombian Andes. *Catena*, 63, 85–108. <https://doi.org/10.1016/j.catena.2005.05.012>
- Inam, S. (2021). Effect of tourism on small business in Lulusar-Dudipat National Park (LDNP) Kaghan Valley, District Mansehra: A comparative study. *International Journal of Business and Management Sciences*, 2(2), 57–67. <https://www.ijbms.org/index.php/ijbms/article/view/53>. Accessed 20 May 2023.
- Jadhao, V. G., Pandey, A., & Mishra, S. K. (2023). Modeling of rain erosivity employing simulated rainfall and laser precipitation monitor. *Modeling Earth Systems and Environment*, 1–16. <https://doi.org/10.1007/s40808-023-01727-0>
- Kalhor, N. A., He, Z., Li, L., Xu, D., Jun, W., Zeb, A., & Khaskheli, N. (2021). Spatial and temporal variations of hydrodynamics and sediment dynamics in Indus River Estuary, Pakistan. *Global Nest Journal*, 23, 572–580. <https://doi.org/10.30955/gnj.003333>
- Karydas, C., Bouarour, O., & Zdruli, P. (2020). Mapping spatio-temporal soil erosion patterns in the Candelaro River Basin, Italy, using the G2 model with Sentinel2 imagery. *Geosciences*, 10, 89. <https://doi.org/10.3390/geosciences10030089>
- Kayet, N., Pathak, K., Chakrabarty, A., & Sahoo, S. (2018). Evaluation of soil loss estimation using the RUSLE model and SCS-CN method in hillslope mining areas. *International Soil and Water Conservation Research*, 6, 31–42. <https://doi.org/10.1016/j.iswcr.2017.11.002>
- Khan, A. (2021). Quantification of soil erosion by integrating geospatial and Revised Universal Soil Loss Equation in District Dir Lower, Pakistan: Soil erosion estimation using RUSLE model. Proceedings of the Pakistan Academy of Sciences: B. *Life and Environmental Sciences*, 58, 17–28. [https://doi.org/10.53560/PPASB\(58-4\)678](https://doi.org/10.53560/PPASB(58-4)678)
- Khwaja, M. A., Saeed, S., & Urooj, M. (2018). *Preliminary environmental impact assessment (EIA) study of China-Pakistan economic corridor (CPEC) northern route road construction activities in Khyber Pakhtunkhwa (KPK), Pakistan*. SDPI, Pakistan.
- Kim, S. M., Choi, Y., Suh, J., Oh, S., Park, H. D., & Yoon, S. H. (2012). Estimation of soil erosion and sediment yield from mine tailing dumps using GIS: A case study at the Samgwang mine, Korea. *Geosystem Engineering*, 15, 2–9. <https://doi.org/10.1080/12269328.2012.674426>
- Koirala, P., Thakuri, S., Joshi, S., & Chauhan, R. (2019). Estimation of soil erosion in Nepal using a RUSLE modeling and geospatial tool. *Geosciences*, 9, 147. <https://doi.org/10.3390/geosciences9040147>
- Lal, R. (2001). Soil degradation by erosion. *Land Degradation & Development*, 12(6), 519–539. <https://doi.org/10.1002/ldr.472>

- Lal, R. (2003). Soil erosion and the global carbon budget. *Environment International*, 29(4), 437–450. [https://doi.org/10.1016/S0160-4120\(02\)00192-7](https://doi.org/10.1016/S0160-4120(02)00192-7)
- Li, Z., & Fang, H. (2016). Impacts of climate change on water erosion: A review. *Earth-Science Reviews*, 163, 94–117. <https://doi.org/10.1016/j.earscirev.2016.10.004>
- Li, L., Zhu, W., Liu, J., Zhang, L., Zhu, L., Wang, L., & Gurung, S. B. (2022). Study on multidimensional changes of rainfall erosivity during 1970–2017 in the North–South Transition Zone, China. *Frontiers in Environmental Science*, 10, 2164. <https://doi.org/10.3389/fenvs.2022.969522>
- Liou, Y. A., Nguyen, Q. V., Hoang, D. V., & Tran, D. P. (2022). Prediction of soil erosion and sediment transport in a mountainous basin of Taiwan. *Progress in Earth and Planetary Science*, 9, 1–15. <https://doi.org/10.1186/s40645-022-00512-4>
- Luetzenburg, G., Bittner, M. J., Calsamiglia, A., Renschler, C. S., Estrany, J., & Poeppl, R. (2020). Climate and land use change effects on soil erosion in two small agricultural catchment systems Fugnitz–Austria, Can Revull–Spain. *Science of the Total Environment*, 704, 135389. <https://doi.org/10.1016/j.scitotenv.2019.135389>
- Mahala, A. (2020). Land degradation processes of Silabati river basin, West Bengal, India: A physical perspective. In R. B. Singh, M. D. Pant & J. L. Raj (Eds.), *Gully Erosion Studies from India and Surrounding Regions* (pp. 299–313). Cham: Springer International Publishing.
- Maqsoom, A., Aslam, B., Hassan, U., Kazmi, Z. A., Sodangi, M., Tufail, R. F., & Farooq, D. (2020). Geospatial assessment of soil erosion intensity and sediment yield using the revised universal soil loss equation (RUSLE) model. *ISPRS International Journal of Geo-Information*, 9, 356. <https://doi.org/10.3390/ijgi9060356>
- Maurya, N. K., & Tanwar, P. S. (2021). Estimation of temporal R-factor based on monthly precipitation data. In *Journal of Physics: Conference Series Vol. 2070, No. 1*, p. 012210. IOP Publishing. <https://doi.org/10.1088/1742-6596/2070/1/012210>
- Meadows, M. E. (2003). Soil erosion in the Swartland, Western Cape Province, South Africa: Implications of past and present policy and practice. *Environmental Science and Policy*, 6, 17–28. [https://doi.org/10.1016/S1462-9011\(02\)00122-3](https://doi.org/10.1016/S1462-9011(02)00122-3)
- Millington, A. C. (1986). Reconnaissance scale soil erosion mapping using a simple geographic information system in the humid tropics. In J. C. De Blij & T. B. H. W. Abebaw (Eds.), *Land Evaluation for Land-Use Planning and Conservation in Sloping Areas* (pp. 64–81). ISSS FAO ITC.
- Mitasova, H., Barton, C. M., Ullah, I., Hofierka, J., & Harmon, R. S. (2013). *GIS-based soil erosion modeling. In Remote sensing and GIScience in geomorphology* (pp. 228–258). Elsevier Inc.. <https://doi.org/10.1016/B978-0-12-374739-6.00052-X>
- Moore, I. D., & Burch, G. J. (1986). Physical basis of the length-slope factor in the universal soil loss equation. *Soil Science Society of America Journal*, 50, 1294–1298. <https://doi.org/10.2136/sssaj1986.03615995005000050042x>
- Morgan, R. P. (2009). *Soil erosion and conservation*. John Wiley & Sons.
- Musabbir, M., Islam, A. R. M. T., Rahman, M. S., Pal, S. C., Alam, E., & Mallick, J. (2023). Spatiotemporal variability of rainfall erosivity and its teleconnection with atmospheric circulation in monsoon-driven climate region. *Catena*, 221, 106762. <https://doi.org/10.1016/j.catena.2022.106762>
- Neupane, B. K., Mandal, U. K., Al-Quraishi, A. M. F., Ozdemir, M., & Rai, R. (2023). Environmental threat of soil erosion in the Gwang Khola Watershed, Chure Region of Nepal. *Iraqi Geological Journal*, 56(1E), 194–206. <https://doi.org/10.46717/igj.56.1E.14ms-2023-5-24>
- Obiahu, O. H., & Elias, E. (2020). Effect of land use land cover changes on the rate of soil erosion in the Upper Eyiohia river catchment of Afikpo North Area, Nigeria. *Environmental Challenges*, 1, 100002. <https://doi.org/10.1016/j.envc.2020.100002>
- Osman, K. T., & Osman, K. T. (2014). Soil erosion by water. In R. Lal (Ed.), *Soil degradation, conservation and remediation* (pp. 69–101). Springer Netherlands.
- Panagos, P., Ballabio, C., Borrelli, P., Meusburger, K., Klik, A., Rousseva, S., & Alewell, C. (2015a). Rainfall erosivity in Europe. *Science of the Total Environment*, 511, 801–814. <https://doi.org/10.1016/j.scitotenv.2015.01.008>
- Panagos, P., Borrelli, P., & Meusburger, K. (2015b). A new European slope length and steepness factor (LS-Factor) for modeling soil erosion by water. *Geosciences*, 5, 117–126. <https://doi.org/10.3390/geosciences5020117>
- Panagos, P., Borrelli, P., Meusburger, K., Yu, B., Klik, A., Jae Lim, K., & Ballabio, C. (2017). Global rainfall erosivity assessment based on high-temporal resolution rainfall records. *Scientific Reports*, 7, 4175. <https://doi.org/10.1038/s41598-017-04282-8>
- Park, S., Oh, C., Jeon, S., Jung, H., & Choi, C. (2011). Soil erosion risk in Korean watersheds, assessed using the revised universal soil loss equation. *Journal of Hydrology*, 399, 263–273. <https://doi.org/10.1016/j.jhydrol.2011.01.004>
- Patriche, C. V., Roşca, B., Pîrnău, R. G., Vasiliniuc, I., & Irimia, L. M. (2023). Simulation of rainfall erosivity dynamics in Romania under climate change scenarios. *Sustainability*, 15, 1469. <https://doi.org/10.3390/su15021469>
- Piacentini, T., Galli, A., Marsala, V., & Miccadei, E. (2018). Analysis of soil erosion induced by heavy rainfall: A case study from the NE Abruzzo Hills Area in Central Italy. *Water*, 10, 1314. <https://doi.org/10.3390/w10101314>
- Pradeep, G. S., Krishnan, M. N., & Vijith, H. (2015). Identification of critical soil erosion prone areas and annual average soil loss in an upland agricultural watershed of Western Ghats, using analytical hierarchy process (AHP) and RUSLE techniques. *Arabian Journal of Geosciences*, 8, 3697–3711. <https://doi.org/10.1007/s12517-014-1460-5>
- Qaisar, M., Shah, M. D., Mahmood, T., Khan, K., Iqbal, T., & Ahmad, N. (2008). Kaghan Valley (Pakistan) earthquakes of February 14, 2004: Source mechanism, intensity distribution and their impact. *Journal of Himalayan Earth Sciences*, 41, 19–32.
- Rawat, K. S., & Singh, S. K. (2018). Appraisal of soil conservation capacity using NDVI model-based C factor of RUSLE model for a semi-arid ungauged watershed: A case study. *Water Conservation Science and Engineering*, 3, 47–58. <https://doi.org/10.1007/s41101-018-0042-x>
- Raza, A., Farooqi, A., Javed, A., & Ali, W. (2016). Distribution, enrichment, and source identification of selected heavy metals in surface sediments of the Siran River, Mansehra, Pakistan. *Environmental monitoring and assessment*, 188, 1–15. <https://doi.org/10.1007/s10661-016-5586-7>

- Renard, K. G., Foster, G. R., Weesies, G. A., McCool, D. K., & Yoder, D. C. (1996). Predicting soil erosion by water: A guide to conservation planning with the Revised Universal Soil Loss Equation (RUSLE). *Agriculture handbook*, 703, 25–28.
- Sharpley, A. N., Williams, J. R., & (EDS.). (1990). *EPIC erosion/productivity impact calculator: 1* (p. 1768). Bull: Model Documentation. USDA Tech.
- Shin, G. J. (1999). *The analysis of soil erosion analysis in watershed using GIS*. Department of Civil Engineering, Gang-won National University, Gangwon-do, South Korea, Ph. D. dissertation.
- Swarnkar, S., Malini, A., Tripathi, S., & Sinha, R. (2018). Assessment of uncertainties in soil erosion and sediment yield estimates at ungauged basins: an application to the Garra River basin, India. *Hydrology and Earth System Sciences*, 2471–2485. <https://doi.org/10.5194/hess-22-2471-2018>
- Taneez, M., Jamil, S., & Ramzan, M. (2021). Water quality assessment and identification of pollution risk in high-altitude saiful muluk lake, north east, Pakistan. *Water, Air, and Soil Pollution*, 232, 230. <https://doi.org/10.1007/s11270-021-05191-3>
- Tiruneh, G., & Ayalew, M. (2015). Soil loss estimation using geographic information system in enfrac watershed for soil conservation planning in highlands of Ethiopia. *International Journal of Agricultural Research. Innovation and Technology (IJARIT)*, 5, 21–30. <https://doi.org/10.3329/ijarit.v5i2.26265>
- Toubal, A. K., Achite, M., Ouillon, S., & Dehni, A. (2018). Soil erodibility mapping using the RUSLE model to prioritize erosion control in the Wadi Sahouat basin, North-West of Algeria. *Environ Monit Assess*, 190, 210. <https://doi.org/10.1007/s10661-018-6580-z>
- Ul-Hussan, W., Khurram Shahzad, M., Seidel, F., Costa, A., & Nestmann, F. (2020). Comparative assessment of spatial variability and trends of flows and sediments under the impact of climate change in the Upper Indus Basin. *Water*, 12, 730. <https://doi.org/10.3390/w12030730>
- Ullah, S., Ali, A., Iqbal, M., Javid, M., & Imran, M. (2018). Geospatial assessment of soil erosion intensity and sediment yield: A case study of Potohar Region, Pakistan. *Environmental Earth Sciences*, 77, 1–13. <https://doi.org/10.1007/s12665-018-7867-7>
- Usovich, B., Lipiec, J., Łukowski, M., & Słomiński, J. (2021). Improvement of spatial interpolation of precipitation distribution using cokriging incorporating rain-gauge and satellite (SMOS) soil moisture data. *Remote Sensing*, 13(5), 1039. <https://doi.org/10.3390/rs13051039>
- Walling, D. E. (1983). The sediment delivery problem. *Journal of Hydrology*, 209–237. [https://doi.org/10.1016/0022-1694\(83\)90217-2](https://doi.org/10.1016/0022-1694(83)90217-2)
- Wallingford, T. C. I. H. (1998). *Tarbela Dam sediment management study* (p. 2). Lahore, Pakistan.
- Wan, W., Liu, Z., Li, B., Fang, H., Wu, H., & Yang, H. (2022). Evaluating soil erosion by introducing crop residue cover and anthropogenic disturbance intensity into cropland C-factor calculation: Novel estimations from a cropland-dominant region of Northeast China. *Soil and Tillage Research*, 219, 105343. <https://doi.org/10.1016/j.still.2022.105343>
- Wischmeier, W. H., & Smith, D. D. (1978). *Predicting rain-fall erosion losses: A guide to conservation planning (No. 537)*. Department of Agriculture, Science and Education Administration.
- Wischmeier, W. H., Johnson, C. B., & Cross, B. V. (1971). Soil erodibility nomograph for farmland and construction sites. *Journal of Soil and Water Conservation*, 26, 189–193.
- Xie, W., Li, X., Jian, W., Yang, Y., Liu, H., Robledo, L. F., & Nie, W. (2021). *A novel hybrid method for landslide susceptibility mapping-based geo detector and machine learning cluster: A case of Xiaojin county, China* (Vol. 10, p. 93). ISPRS International Journal of Geo-Information. <https://doi.org/10.3390/ijgi10020093>
- Yan, F. L., Shi, Z. H., Li, Z. X., & Cai, C. F. (2008). Estimating inter rill soil erosion from aggregate stability of Ultisols in subtropical China. *Soil and Tillage Research*, 100, 34–41. <https://doi.org/10.1016/j.still.2008.04.006>
- Yuliang, Q., & Yun, Q. (2002). Fast soil erosion investigation and dynamic analysis in the loess plateau of China by using information composite technique. *Advances in Space Research*, 29, 85–88. [https://doi.org/10.1016/s0273-1177\(01\)00633-0](https://doi.org/10.1016/s0273-1177(01)00633-0)
- Zaidi, A. Z., & Khan, M. (2018). Identifying high potential locations for run-of-the-river hydroelectric power plants using GIS and digital elevation models. *Renewable and Sustainable Energy Reviews*, 89, 106–116. <https://doi.org/10.1016/j.rser.2018.02.025>
- Ziadat, F. M., & Taimeh, A. Y. (2013). Effect of rainfall intensity, slope, land use and antecedent soil moisture on soil erosion in an arid environment. *Land Degradation and Development*, 24, 582–590. <https://doi.org/10.1002/ldr.2239>

Recommendation The Surface Water Hydrology Department of WAPDA operates gauging stations on nearly all of Pakistan's major rivers. The data from these gauging stations can be utilized to learn more about the suspended sediment load carried by rivers and, eventually, reservoir sedimentation. Additional studies on soil erosion utilizing geospatial technology are needed, to identify areas that are vulnerable to soil erosion so that area-specific remedies can be implemented. Additional research is suggested due to the huge potential for diverse hydrologic, climatological, ecological, and statistical modeling applications in soil erosion investigations. It is recommended that the impact of specific causal components, such as land use, rainfall, and vegetation cover, be investigated at the watershed level.

Publisher's Note Springer Nature remains neutral with regard to jurisdictional claims in published maps and institutional affiliations.

Springer Nature or its licensor (e.g. a society or other partner) holds exclusive rights to this article under a publishing agreement with the author(s) or other rightsholder(s); author self-archiving of the accepted manuscript version of this article is solely governed by the terms of such publishing agreement and applicable law.